massDOT
Massachusetts Department of Transportation

June 2022
Report No. 22-030

A Pavement Marking Inventory and Retroreflectivity Condition Assessment Method Using Mobile LiDAR

Principal Investigator (s)
Dr. Chengbo Ai

University of Massachusetts Amherst

Research and Technology Transfer Section
MassDOT Office of Transportation Planning

U.S. Department of Transportation
Federal Highway Administration

[This blank page will be the back of your front cover]

Technical Report Document Page

1. Report No.	2. Government Accession No.	3. Recipient's Catalog No.
22-030		

4. Title and Subtitle	5. Report Date
A Pavement Marking Inventory and Retroreflectivity Condition Assessment Method Using Mobile LiDAR	June 2022
	6. Performing Organization Code
7. Author(s)	8. Performing Organization Report No.
Chengbo Ai and Emily Hennessy	22-030
9. Performing Organization Name and Address	10. Work Unit No. (TRAIS)
University of Massachusetts Amherst 130 Natural Resources Way, Amherst, MA 01003	11. Contract or Grant No.
12. Sponsoring Agency Name and Address	13. Type of Report and Period Covered
Massachusetts Department of Transportation Office of Transportation Planning Ten Park Plaza, Suite 4150, Boston, MA 02116	Final Report June 2022 [February 2020–June 2022]
	14. Sponsoring Agency Code n/a

15. Supplementary Notes
Project Champion - Neil Boudreau, MassDOT

16. Abstract

FHWA is proposing regulations to guide minimum pavement marking retroreflectivity levels, which poses a potential challenge to MassDOT, as the current practice of visual inspection is labor-intensive, and the results can be subjective. To address the identified challenges and needs from MassDOT, the objective of this research is twofold: (1) to serve as a proof of concept for the use of mobile LiDAR to locate and assess the pavement markings for selected testing sections by developing and evaluating new automated LiDAR processing algorithms, and (2) to investigate the feasibility of identifying deterioration trend of retroreflectivity condition. This study has developed a complete pavement marking inventory with retroreflectivity conditions for the 14 selected testing sections and also compared historical and current data to inform the deterioration trends of three types of marking materials, including polyurea, epoxy, and thermoplastic. The findings of this study will guide the future phases of the study with a larger selection of testing sections, material types, and roadway characteristics. The outcomes of the series of studies will help better define the benefit-to-cost ratio for different marking materials and eventually lead to the development of MassDOT's pavement marking standard.

17. Key Word	18. Distribution Statement
Pavement markings, LiDAR, retroreflectivity condition assessment, benefit-to-cost ratio	

19. Security Classif. (of this report)	20. Security Classif. (of this page)	21. No. of Pages	22. Price
unclassified	unclassified	56	n/a

Form DOT F 1700.7 (8-72) Reproduction of completed page authorized

This page left blank intentionally.

A Pavement Marking Inventory and Retroreflectivity Condition Assessment Method Using Mobile LiDAR

Final Report

Prepared By:

Chengbo Ai, PhD
Principal Investigator

Emily Hennessey
Graduate Researcher

The University of Massachusetts Amherst,
130 Natural Resources Rd., Amherst, MA 01003

Prepared For:

Massachusetts Department of Transportation
Office of Transportation Planning
Ten Park Plaza, Suite 4150
Boston, MA 02116

June 2022

This page left blank intentionally.

Acknowledgments

Prepared in cooperation with the Massachusetts Department of Transportation, Office of Transportation Planning, and the United States Department of Transportation, Federal Highway Administration.

The Project Team would like to acknowledge the efforts of Mr. Neil Boudreau, Mr. James Danila, Mr. Noah Thompson from the Highway Division at MassDOT for providing technical support and oversight for this project, and Dr. Lily Oliver, Mr. Nicholas Zavolas from the Office of Transportation Planning at MassDOT, for providing necessary data and constructive suggestions for this project.

The Project Team would also like to acknowledge the effort of Mr. Matt Mann and Ms. Kimberley Foster from the University of Massachusetts Transportation Center for their administrative support.

Disclaimer

This page left blank intentionally.

Executive Summary

This study of "A Pavement Marking Inventory and Retroreflectivity Condition Assessment Method Using Mobile LiDAR" was undertaken as part of the Massachusetts Department of Transportation (MassDOT) Research Program. This program is funded with Federal Highway Administration (FHWA) State Planning and Research (SPR) funds. Through this program, applied research is conducted on topics of importance to the Commonwealth of Massachusetts transportation agencies.

This study is aimed at utilizing mobile light detection and ranging (LiDAR) and video log imagery data and developing an automated method for the extraction, localization, and retroreflectivity condition assessment of in-service pavement markings. The research team selected 14 representative testing sections with various road characteristics, pavement marking materials, and installation times, for analysis in this study. The detailed objectives include:

- Develop and validate an automated method for the inventory and retroreflectivity condition assessment for pavement markings as a proof of concept by leveraging the mobile LiDAR and video log images.
- Investigate the feasibility of identifying deterioration trends of retroreflectivity conditions using the developed LiDAR-based method for better defining the benefit-to-cost ratio of different pavement marking materials in the future and eventually leading toward the MassDOT's pavement marking standards.

The deliverables of this study include a complete, georeferenced pavement marking inventory with retroreflectivity condition measurements for the 14 selected road sections. The georeferenced inventory database also includes the retroreflectivity deterioration trends covering three observation timestamps (i.e., 6-month intervals) within the duration of this study.

The outcome of this study is summarized as follows:

- *A Review of Pavement Marking Efforts*. The research team conducted a detailed literature review of available and ongoing research through Transport Research International Documentation (TRID) on pavement marking inventory and condition evaluation methods and mobile LiDAR applications in pavement marking studies.
- *Mobile LiDAR Data Acquisition*. The research team conducted a comprehensive data acquisition and data preprocessing using the mobile LiDAR sensor (i.e., Riegl VMZ-2000) along with the 14 selected testing sections. The LiDAR data collected in 2016 by MassDOT was also incorporated into the final dataset.

- The collected data cover more than 70 miles of different classifications of highways, with different pavement marking material types.
- For each testing section, three data collections were conducted at a 6-month interval to monitor the deterioration of the pavement markings.
- Addition data collection with mobile LiDAR, handheld retroreflectometer, and mobile retroreflectometer was conducted at the beginning of the study for the method development and result validation.

- *Automated Pavement Marking Extraction*. The research team developed an automated pavement marking extraction algorithm based on the existing effort by the Oregon Department of Transportation and Oregon State University using the Road Marking Extractor (RoME). This new automated pavement marking extraction algorithm was customized to fit the workflow of this study, including the longitudinal line extraction, break line linkage, and noise reduction. The developed algorithm is used to identify the delineations of the pavement markings in the 14 testing sections and establish the spatial references in the final inventory database.
- *Automated Pavement Marking Retroreflectivity Condition Evaluation*. The research team developed an automated pavement marking retroreflectivity condition evaluation method through the correlation between the retro-intensity from mobile LiDAR and the retroreflectivity measurements from handheld/mobile retroreflectometer. A customized normalization scheme was created to rectify the retro-intensity measurements based on the distance and incidence angle of the LiDAR scanning beam.
    - The research team validated the repeatability and accuracy of the developed method. The results demonstrated a close correlation with the mobile retroreflectometer and superior repeatability over the mobile retroreflectometer. The disparity between the developed method and the mobile retroreflectometer measurements was attributed to the mismatch of locations from both methods.
    - The research team incorporated the surface material loss into the pavement marking inventory results. The material loss is not only an important condition indicator for pavement markings; it is identified that the percentage loss also played an important role in determining retroreflectivity conditions, especially for materials that may experience binding failure due to age and fatigue.
- *Pavement Marking Retroreflectivity Condition Deterioration*. The research team utilized the developed automated algorithms and methods and investigated the deterioration trends for the three pavement marking materials in the selected testing sections, including polyurea, epoxy, and thermoplastic. With three 6-month observation windows, initial deterioration trends were established, and the difference in materials was investigated.

- At comparable AADT levels, deterioration rates varied among three tested materials: 1) polyurea has a minimum annual deterioration of less than 10 mcd/m^2/lux; epoxy has a consistent annual deterioration of around 10 mcd/m^2/lux; 3) thermoplastic has a much larger deterioration of 20-30 mcd/m^2/lux.
- Regardless of the installation locations and years, deterioration variability was observed differently for the three tested materials: 1) polyurea and epoxy have a small deterioration variability along the same testing section at less than 5 mcd/m^2/lux; 2) thermoplastic material has much larger variability among the same testing section at 10-15 mcd/m^2/lux. While the variability may be attributed to other factors like installation inhomogeneity, a further investigation of the surface percentage loss revealed that the variability of retroreflectivity change can be attributed to the loss of binding material instead of the loss of reflective material.

- *Pavement Marking Management using LiDAR*. The research team has developed a complete methodology for automatically inventorying the location of the in-service pavement markings and evaluating their corresponding retroreflectivity condition and binding material loss, leveraging mobile LiDAR and video log imagery data. While further analysis is recommended for waterborne and preformed tape material, recessed marking, and raised pavement markers (RPMs), the outcomes of this study have demonstrated that the mobile LiDAR-based method is a feasible and reliable option for state transportation agencies to implement in their pavement marking inventory and retroreflectivity condition evaluation program.

This page left blank intentionally.

Table of Contents

This page left blank intentionally.

List of Figures

This page left blank intentionally.

List of Acronyms

Acronym	Expansion
AADT	Annual Average Daily Traffic
AASHTO	American Association of State Highway and Transportation Officials
ASTM	American Society of Testing and Materials
CAV	connected and autonomous vehicles
FHWA	Federal Highway Administration
GIS	Geographic Information System
GPS	Global Positioning System
IMU	Inertial Measurement Unit
INS	Inertial Navigation System
LiDAR	Light Detection and Ranging
MassDOT	Massachusetts Department of Transportation
MUTCD	Manual on Uniform Traffic Control Devices
NCHRP	National Cooperative Highway Research Program
RoME	Road Marking Extractor
RPM	Raised Pavement Marker
SPR	State Planning and Research
TRID	Transport Research International Documentation

This page left blank intentionally.

1.0 Introduction

This study of "A Pavement Marking Inventory and Retroreflectivity Condition Assessment Method Using Mobile LiDAR" was undertaken as part of the Massachusetts Department of Transportation (MassDOT) Research Program. This program is funded with Federal Highway Administration (FHWA) State Planning and Research (SPR) funds. Through this program, applied research is conducted on topics of importance to the Commonwealth of Massachusetts transportation agencies.

1.1 Background

Pavement markings are a vital transportation asset and traffic control device which facilitates safe and predictable driver behaviors. The effectiveness of pavement markings is dependent upon their condition, particularly during nighttime and adverse weather, and MassDOT continues actively pursuing new and more durable marking materials. To improve marking performance at a national level, FHWA is proposing regulations to guide minimum pavement marking retroreflectivity levels. Regulatory compliance poses a challenge, as conventional methods of visual inspection are labor-intensive, and the results can be subjective. There is a pressing need for MassDOT to develop and implement an effective, efficient inventory and reliable retroreflectivity condition assessment method for pavement marking.

With the fast-paced advancements in mobile data acquisition and machine learning in recent years, automated roadway assets detection and recognition algorithms using mobile light detection and ranging (LiDAR) have become a feasible option for inventorying critical traffic control devices. As many state DOTs, including MassDOT, have been actively collecting mobile LiDAR data, the accumulated point cloud data has become an excellent data repository to support the development of these algorithms. However, the accumulation of these LiDAR data results in creating an intensive data processing and management burden. Therefore, there is an emerging need for MassDOT to leverage the existing and incoming LiDAR point cloud data and develop an effective pavement marking inventory and condition assessment method.

In previous studies, researchers and practitioners have made an extensive effort to explore and develop effective and efficient methods for pavement marking inventory and, more importantly, retroreflectivity condition evaluation. However, two primary limitations have been identified from previous studies:

- The existing retroreflectivity measuring devices, including the handheld retroreflectometer and the mobile retroreflectometer, have been widely employed in the evaluation of the pavement marking retroreflectivity condition. However, these devices and methods still encountered challenges in obtaining consistent retroreflectivity measurements to better understand the temporal deterioration of the marking due to the sparse sampling for measurements, and the measurement instability from the devices, respectively.
- While there were a limited number of attempts on automated pavement marking inventory or retroreflectivity condition assessments in previous studies, limited effort has been focused on exploring the feasibility of using mobile LiDAR for developing accurate and consistent pavement marking inventory.

This study, as a proof of concept, is aimed to build the foundation of establishing an automated LiDAR-based methodology/program for comprehensively building the pavement marking management program. The findings of this study are expected to guide MassDOT's selection of marking materials and repair frequency. In addition, with the complete pavement marking inventory and condition information, the outcome of this study will also establish an essential data layer to support MassDOT's decisions on connected and autonomous vehicles (CAV) testing, implementation, and operation.

1.2 Objectives and Detailed Work Tasks

This study is aimed at utilizing mobile light detection and ranging (LiDAR) and video log imagery data and developing an automated method for the extraction, localization, and retroreflectivity condition assessment of in-service pavement markings. The research team selected 14 representative testing sections with various road characteristics, pavement marking materials, and installation times, for analysis within this study. The detailed objectives include:

- Develop and validate an automated method for the inventory and retroreflectivity condition assessment for pavement markings as a proof of concept by leveraging the mobile LiDAR and video log images.
- Investigate the feasibility of identifying deterioration trends of retroreflectivity conditions using the developed LiDAR-based method for better defining the benefit-to-cost ratio of different pavement marking materials in the future and eventually leading toward the MassDOT's pavement marking standards.

The deliverables of this study include a complete, georeferenced pavement marking inventory with retroreflectivity condition measurements for the 14 selected road sections. The georeferenced inventory database also includes the retroreflectivity deterioration trends

covering three observation timestamps (i.e., 6-month intervals) within the duration of this study. The detailed tasks completed in this study are listed as follows:

- *Task 1 - Review of Pavement Marking Inventory and Condition Evaluation Efforts*: The research team conducted a detailed literature review of available and ongoing research and implementation efforts for pavement marking inventory and retroreflectivity condition evaluation that have been made by MassDOT, other transportation agencies, and the research community.
- *Task 2 - Mobile LiDAR Data Acquisition*: The research team conducted a comprehensive data acquisition and data preprocessing using the mobile LiDAR sensor (i.e., Riegl VMZ-2000) along with the 14 selected testing sections, covering more than 70 miles of different classifications of highways, with different pavement marking material types. For each testing section, three data collections were conducted at a 6-month interval to monitor the deterioration of the pavement markings.
- *Task 3 - Mobile LiDAR Data Processing for the Baseline Data*: The research team developed and applied automated LiDAR-based algorithms for extracting the locations of pavement markings and evaluating the retroreflectivity conditions for the identified road sections using the baseline data from 2016.
- *Task 4 - Mobile LiDAR Data Processing for the Updated Data*: The research team developed and applied automated LiDAR-based algorithms for extracting the location of pavement markings and evaluating the retroreflectivity conditions for the identified 14 testing sections using the newly collected data in this study.
- *Task 5 - Pavement Marking Retroreflectivity Condition Deterioration Evaluation*: The research team utilized the developed automated algorithms and methods and investigated the deterioration trends for the three pavement marking materials in the selected testing sections, including polyurea, epoxy, and thermoplastic. With three 6-month observation windows, initial deterioration trends were established, and the difference in materials was investigated.
- *Task 6 - Reporting of Results:* The research team prepared the final report and the corresponding PowerPoint-based project presentation with all the technical details.

1.3 Organization of this Report

This report is organized as follows. Section 1 introduces the background, research needs, objectives, and the detailed work tasks of this research project. Section 2 presents the proposed method, including the literature review, the developed algorithms for processing mobile LiDAR data for inventory and retroreflectivity condition information extraction, and

the investigation of the deterioration trends of different pavement marking materials. Section 3 presents the results of the proposed method. Section 4 summarizes the findings and results of this project and recommendations for future studies.

2.0 Research Methodology

The research methodology for this study consisted of three main parts: a review of existing data and technologies, collection of the mobile LiDAR data, and the processing of the mobile LiDAR data for pavement marking inventory and condition assessment. Section 2.1 presents a review of the literature related to the existing effort for pavement marking inventory and retroreflectivity condition assessment methods. Section 2.2 presents an overview of the research methodology, followed by Sections 2.3 through 2.6 that describe the methods for mobile LiDAR data acquisition and processing for pavement marking extraction, retroreflectivity condition evaluation, and surface condition evaluation.

2.1 Literature Review

2.1.1 Pavement Markings

Vehicle crashes and fatalities are overrepresented during the nighttime. Half of all traffic fatalities occur during the night, and only a quarter of total travel occurs during that time *(1)*. As such, it is important to monitor, improve, and maintain the roadway infrastructure that aids nighttime traffic safety. Research shows that the retroreflectivity of pavement markings and signs increases the distance of visibility and clarity of perception for drivers at night *(2,3)*.

The *Manual on Uniform Traffic Control Devices* (MUTCD) notes that the visibility of pavement markings can be adversely impacted by snow, debris, and water on or near the markings. Oregon DOT has identified several factors which influence the visibility of pavement markings which include: infrastructure condition, pavement marking locations, placement quality, usage, material, color, contrast, design, condition, configuration, width, pattern, raised pavement markers, retroreflectivity, and local snow removal practices *(4)*. The increased width of pavement markings and continuous markings have been linked with increased driver sight distances *(3)*.

These limitations to the perception of pavement markings describe a large number of variables that could contribute to a traffic crash, including the retroreflectivity of the markings. This literature review discusses pavement markings, retroreflectivity, and mobile LiDAR in an effort to illuminate the asset management potential for mobile LiDAR to assess the pavement marking conditions across a transportation network.

The pavement marking materials used vary based on the anticipated conditions on the roadways and the budget of the managing agency. Paints, thermoplastics, and tapes are very

common and can be supplemented with raised pavement markers and colored markings. The guidance provided by the MUTCD for material selection states that the materials should maintain their specified color throughout their life cycle and that markings should not contribute to a loss of vehicle traction in the roadway *(5)*.

The MUTCD also states that "Markings that must be visible at night shall be retroreflective unless ambient illumination assures that the markings are adequately visible. All markings on Interstate highways shall be retroreflective" *(5)*. Guidance is provided for retroreflective raised pavement markings with respect to spacing and design. Section 3A.03 intends to provide guidance on maintaining minimum pavement marking retroreflectivity but has been reserved for future text. In the forthcoming MUTCD, FHWA has been directed to move forward with establishing the minimum retroreflectivity number for pavement marking. The proposed rulemaking was released, and the comment period ended on May 14, 2021.

2.1.2 Retroreflectivity

Due to the conservation of energy, all emitted light is either reflected, absorbed, or transmitted. The percentages of reflection, absorption, and transmission are a function of the material the light reaches. The reflected light from roadway objects is the focus of this research, and it begins with the concept of bi-hemispherical reflectance, which states that reflected light is distributed over all viewing angles. This perspective is important when studying how much-reflected light reaches a driver's eye. The bi-directional reflectance distribution function quantifies this by accounting for the diffusion of reflectivity with two (2) variables that define the direction of the sensor or observer and two (2) variables defining the direction of the light source relative to the normal plane *(6)*.

Reflective cases include retroreflective, perfect diffuse reflection, and perfect specular reflection. Retroreflection reflects light back to the source along the same angle of approach and occurs with glass beads and reflectors, which are designed for this purpose. Diffuse reflection scatters the approaching light equally in all directions and occurs with rough or matte surfaces. Specular reflection reflects light away from the source at an equal angle to that of its approach and occurs with mirrors and reflective metals *(7,8)*. Luminance is a measure of the amount of light in a given area that is visible to an observer from a given viewing angle and is given in candelas per square meter (cd/m^2), while illuminance is the measurement of how much light illuminates a surface. The ratio of luminance to illuminance in units of candelas per square meter per lux ($cd/m^2/lux$) is a measurement of retroreflected luminance *(9)*.

Retroreflectivity is greatly affected by environmental factors. The presence of water during or after rainfall can significantly reduce the retroreflectivity of the objects along the road *(10–12)*. This is due primarily to an increase in specular reflection caused by films of water on retroreflective surfaces *(10,13)*. Additionally, the presence of water causes refraction along with the retroreflective objects, which can change the angle of reflection and reduce the amount of light reflected back at the driver *(8,12,13)*. Water droplets themselves can reflect, absorb, or transmit light internally, which can alter the angles and quality of the light exiting the water droplet. Research efforts have suggested that it may be possible to predict the performance of a retroreflective object in wet conditions based on its performance in dry conditions, but more testing is needed in this area to develop it further *(11)*.

Traffic, maintenance activities, weather, orientation, and precipitation all contribute to the gradual degradation of the retroreflectivity of pavement markings *(9,14)*. The first year of service life for pavement markers sees a loss of 33-40% of initial retroreflectivity, where the loss of wet retroreflectivity occurs at a higher rate than that of dry retroreflectivity *(3)*. As such, the inspection of facilities is necessary to determine the remaining effectiveness of the retroreflective objects and can serve as a cost-saving measure to prevent premature replacement of those objects. Manual visual nighttime inspections and retroreflectometers are two common types of asset inspection.

National Standards or Methodologies

- *FHWA-HRT-07-059*: This report provided guidance for minimum in-service retroreflectivity for longitudinal markings, which increase with higher roadway design speeds *(15)*.
- *FHWA-SA-08-010*: Methods are identified for assessing the economic impacts of minimum retroreflectivity standards by comparing the life-cycle costs of different materials *(16)*.
- *FHWA-2009-0139*: This document proposes updates to the MUTCD regarding minimum retroreflectivity standards with support from current research findings *(17)*.

Standards ASTM D7585-10 and ASTM E1710-18 provide guidance for evaluating the retroreflectivity of pavement markings with hand-operated instruments and a portable retroreflectometer, respectively. These instruments are not oriented for mobile use and primarily serve to check individual locations rather than monitor the infrastructure as a continuous network. ASTM WK3833 is currently still being drafted but seeks to codify the use of traffic-speed mobile retroreflectivity testing for horizontal pavement marking materials. The need to also monitor longitudinal pavement markings with the same methods has yet to be standardized *(18)*. Other ASTM standards outline methods of testing wet retroreflectivity with portable retroreflectometers but also lack mobile testing capabilities.

2.1.3 Mobile LiDAR

LiDAR technology measures distance by emitting laser light and monitoring the reflection of that laser light with a sensor. As these LiDAR devices can be precisely located in space, the three-dimensional imagery created with the sensor is geolocated. It has applications in survey, asset management, and research fields. The scale of the data collected can vary depending on the sensors used and the method of collection employed in the field, ranging from flyovers of entire neighborhoods to crack detection in pavements. This vast expanse of data can be gathered in a fraction of the time it would take to survey similar areas of interest manually. For highly accurate and detailed data, LiDAR collection can be done with multiple passes of the area of study, which improves the geolocation quality, and allows for the averaging of multiple data sets *(19)*.

As previously discussed, traditional retroreflectivity testing requires manual inspection, or individually operated portable tools, which exposes field crews to the dangers of moving traffic. Mobile LiDAR and remote sensing can allow inspectors to analyze a site while driving through it, or standing offsite and observing, respectively. This improved safety metric makes mobile LiDAR inspections very appealing for state DOTs.

In addition to mapping geometric data, LiDAR tracks the intensity of the laser light returned to the sensor, which provides valuable information regarding the reflectivity of objects in the area of study. These intensity values require calibration and processing before they can be used to assess the reflectivity of objects, as they are affected by environmental and procedural variables like laser range, power, and angles, receiver aperture, system, and atmospheric transmittance, and beam divergence *(20–24)*. This calibration was categorized into levels ranging from zero to three by Kashani et al., which include raw intensity (no correction), intensity correction, intensity normalization, and rigorous radiometric calibration. Another method of classification is to separate the methods into theoretical or model-driven approaches and empirical approaches *(25)*.

The theoretical approaches involve manipulating the laser range equation to account for the environmental and procedural variables. Research efforts have led to the development of a variety of laser range equations *(20–22,26–28)*. Because the source and sensor for the lasers are very close together in LiDAR equipment, the intensity output is a measurement of the retroreflectivity of the objects detected. As such, mobile LiDAR equipment functionally serves as a microcosm for retroreflectivity in the driver's eye. Automated methods for identifying the location of pavement markings within these large data sets begin by first extracting the roadway extends from extraneous data beyond the edge of the pavement. Guan et al. reviewed the different extraction methods. They identified that most methods rely on

aspects of roadway geometry, but others have overlaid other data sources like video, maps, and airborne data to verify pavement extents *(29)*.

The results of this data collection are often projected onto a two-dimensional plane for analysis, where detection thresholds are applied to identify pavement markings *(30–35)*. Because of this two-dimensional projection, the results can be skewed by the distance from the sensor to the pavement marking in question. On such occasions, researchers have normalized the intensity values by the distances and angles of these more distant data points *(36–40)*. Rather than adjusting the recorded intensities, some researchers have opted to make the thresholds for detection dynamic with respect to distances and angles *(41,42)*. Once these thresholds have been identified and applied, morphological operators are used to cluster the pixels of the resultant image. Additional parsing has been done to classify the pavement markings by their geometry and orientation *(30–32,36,39,41–43)*. Of these methods reviewed, some successfully classified specific pavement markings. The research of Zhang et al. 2016 successfully classified sixteen (16) varieties of pavement markings with a combination of a linearly modeled intensity correction method and region grow image processing *(36)*.

Researchers have been able to analyze the LiDAR point cloud data directly without image processing. While the precision of the results is better maintained, the processing time and costs were found to be prohibitive in those cases *(38,43–45)*. However, the technology is improving to be able to assess point cloud data efficiently. More recently, Jung et al. used point cloud data to develop an algorithm of marking parameters to identify roadway markings, even when the markings were incomplete or degraded *(46)*. Algorithms have also been developed which extract pavement lane markings from point clouds with an 88% success rate *(47)*. Three-dimensional laser profiling data has been used with 90.8% accuracy to detect and identify different roadway markings, but no condition assessment was completed with this method *(48)*. Mobile LiDAR has been successfully employed to assess the retroreflectivity of roadway signs with a combination of theoretical and empirical techniques *(49,50)*. In the research to date, mobile LiDAR has not been used to determine the condition of pavement markings.

2.1.4 Summary

Thus far, retroreflectivity testing with mobile LiDAR has been undertaken primarily in controlled environments and has produced variable results. Though there are many factors that can impact the quality of the data collected, there is a need for standardization with the approaches for the acquisition and processing of these data to produce reliable results on a network scale. The benefits of this technology for asset management applications have not

been fully realized. Through the use of repeated scans, the functional life cycle of pavement markings can be better understood and managed without potentially premature sweeping replacements.

There is not enough research regarding the calibration of mobile LiDAR for retroreflectivity testing. While radiometric calibration has been discussed in the literature, it has focused either on specific pieces of equipment or on obtaining other types of information. Though helpful, these studies do not directly relate to the task at hand, and research that directly addresses retroreflectivity with a broader range of equipment would assist DOTs with beginning to incorporate mobile LiDAR to this end. There is a need to leverage the capability of mobile LiDAR to study how it can help automatically inspect the retroreflectivity of pavement markings and to monitor its deterioration.

2.2 Overview of the Proposed Methodology

In this study, the research team developed a complete processing methodology for pavement marking condition evaluation. Figure 2.1 shows an overview of the proposed method. For data acquisition, the research team collected comprehensive video log image data, mobile LiDAR point cloud data, and the metadata for the 14 testing sites selected by the MassDOT engineer. For the processing methods, the research team developed three automated algorithms to extract pavement marking from point cloud data, evaluate the corresponding retroreflectivity condition, and extract the surface condition of the corresponding pavement marking from the video log images. The study produces two key outcomes, including the complete inventory of the 14 testing sites with retroreflectivity conditions and the retroreflectivity condition deterioration evaluation based on the distinctive characteristics of the testing sites.

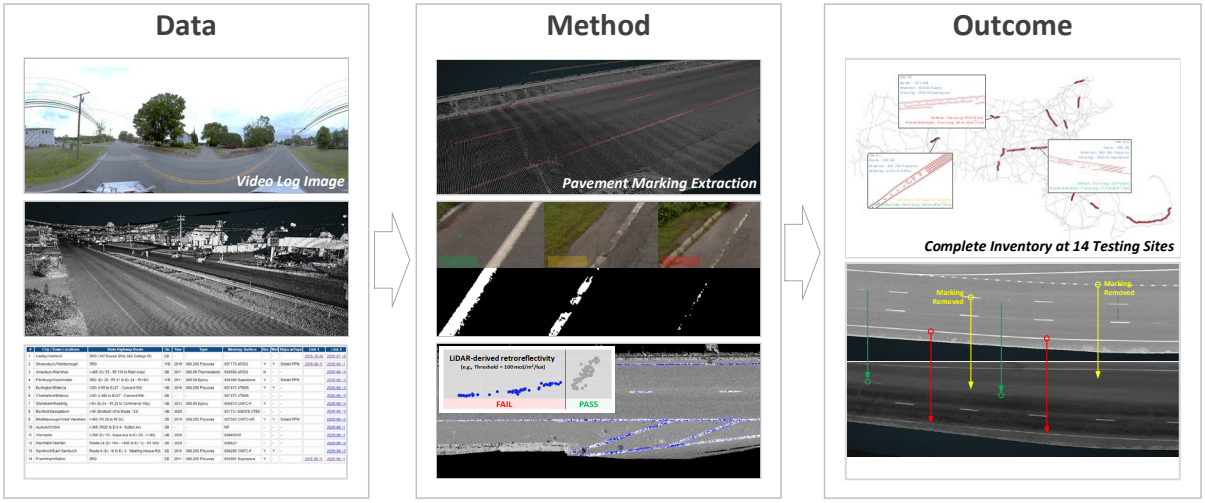

Figure 2.1: Overview of the proposed methodology

2.3 Data Acquisition

In this study, 14 testing sites were selected by MassDOT to include distinctive characteristics of the pavement markings so that the overall feasibility of the LiDAR-based method can be comprehensively conducted. Figure 2.2 shows the details of the selected testing sites and their corresponding locations.

The 14 representative testing sections cover different roadway classifications (including five state highways, three U.S. highways, and six interstates) and different pavement marking materials (including four thermoplastic sections, eight polyurea sections, and two epoxy sections).

#	City / Town Locations	State Highway Route	Dir.	Year	Type	Wearing Surface	Rec.	Wet	Skips w/Tape
1	Hadley/Amherst	SR9 (147 Russel St to 362 College St)	EB	2005	866.06 Termoplastic	6601674	N	N	N
2	Shrewsbury/Westborough	SR9	WB	2018	866.206 Polyurea	607176 ARGG	Y	Y	Slotted RPM
3	Amesbury/Merrimac	I-495 (Ex 55 - Rt 110 to Rest Area)	SB	2011	866.06 Thermoplastic	604586 ARGG	N	N	Slotted RPM
4	Fitchburg/Westminster	SR2 (Ex 28 - Rt 31 to Ex 24 - Rt140)	WB	2011	868.06 Epoxy	604364 Superpave	Y	N	Slotted RPM
5	Burlington/Billerica	US3 (I-95 to Ex27 - Concord Rd)	NB	2015	868.206 Polyurea	607472 UTBO-P and UTBO-AR	Y	Y	N
6	Chelmsford/Billerica	US3 (I-495 to Ex27 - Concord Rd)	SB	2015	868.106 Thermoplastic	607472 UTBO-P and UTBO-A	Y	Y	N
7	Stoneham/Reading	I-93 (Ex34 - Rt 28 to Commerce Way)	NB	2012	868.06 Epoxy	604878 OGFC-P	Y	N	N
8	Boxford/Georgetown	I-95 (Endloott rd to Route 133)	NB	Active	866.06 Thermoplastic	93173 / 608378 UTBO-P	Y	Y	Slotted Tape
9	Middleborough/West Wareham	I-495 (Rt 28 to Rt 58)	SB	2018	868.206 Polyurea	607563 OGFC-AR	Y	Y	Slotted RPM
10	Auburn/Oxford	I-395 (Rt20 to Ext 4 - Sutton Av)	SB	2012	866.206 Polyurea	605585 OGFC	Y	N	Slotted Tape
11	Worcester	I-290 (Ex 10 - Hope Ave to Ex 20 - I-190)	NB	Active	868.206 Polyurea	609400 UTBO-P->SSC-9.5	Y	Y	Slotted Tape
12	Raynham/Taunton	Route 24 (Ex 14A - I-495 to Ex 12 - Rt 140)	SB	Active	868.206 Polyurea	608820	Y	Y	Slotted Tape
13	Sandwich/East Sandwich	Route 6 (Ex 18 to Ex 3 - Meeting House Rd)	EB	2014	868.206 Polyurea	606286 OGFC-P	Y	Y	Slotted RPM
14	Framinham/Natick	SR9	EB	2010	866.206 Polyurea	604991 Superpave – latex mod	Y	N	Slotted RPM

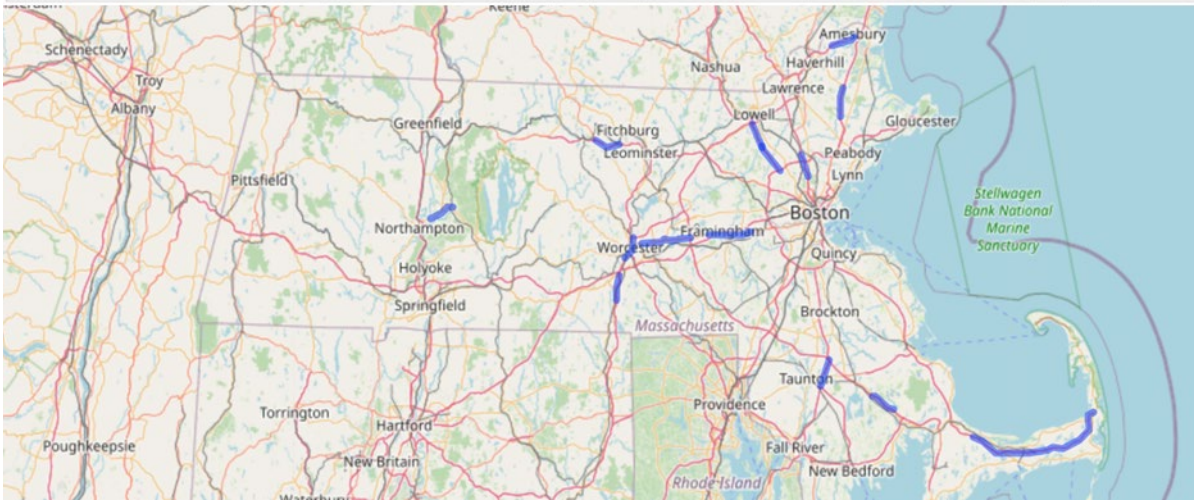

Figure 2.2: Details and locations of the selected testing sites

The data acquisition system used in this study is an integrated mobile LiDAR system, RIEGL VMZ-2000, which consists of three primary components, including the LiDAR sensor, the precise positioning system, and the camera system. Figure 2.3 shows the overview of the data acquisition system used in this study (left: overview; middle: camera and mobile LiDAR; right: control panel). The LiDAR sensor is used to acquire the point cloud of the roadway, including guardrails. Each point consists of the precise position information that is derived from the integrated precise positioning system. The integrated precise positioning system is used to acquire accurate coordinates that are composed of a global positioning system (GPS) and an inertial measurement unit (IMU). The camera system (FLIR Ladybug 5+ camera) is used to capture video log images that are registered to the LiDAR sensor. In this study, the point cloud data acquired by the LiDAR sensor was used for all the data processing steps, including automated pavement marking extraction and retroreflectivity condition evaluation, while the video log images acquired by the camera system were used for pavement marking surface condition extraction.

The current LiDAR sensor can produce 400,000 measurements per second in both the line scanning mode and the radar scanning mode. For the application of the corridor scanning with the best point cloud density, the vertical line scanning mode was selected. Figure 2.3 shows the vertical configurations for the line scanning mode. The scanning line forms a 100° vertical fan to cover the road surface, especially the roadside objects. To acquire the point could with better homogeneity of point cloud densities, the frequency of the LiDAR sensor and the LiDAR heading angle were configured at 75 Hz (i.e., lines per second) and 28° (i.e., the angle of the scanning fan to ground surface).

Figure 2.3: Integrated data collection vehicle

2.4 Pavement Marking Extraction

The objective of pavement marking extraction is to extract pavement markings from the captured point cloud data automatically. The marking-associated point cloud represents the extracted pavement markings. As discussed in the literature review, pavement marking extraction methods using mobile LiDAR have been extensively studied. Therefore, the research team decided to adopt an existing algorithm with satisfactory performance and then customize the processing algorithm instead of developing an automated tool from scratch. After thoroughly exploring and evaluating available algorithms, the research team selected the Road Marking Extractor (RoME) tool developed by Oregon State University (OSU) *(46)* as the underlying algorithm for extracting pavement markings from the collected LiDAR point cloud. Figure 2.4 shows the overview of the RoME algorithm. The research team further calibrated the radiometric of the LiDAR sensor (i.e., Riegl VMZ-2000) used in this study for the subsequent retroreflectivity measurement. The details of the developed algorithm can be referred to in the project report and the publication by the OSU team *(2)*.

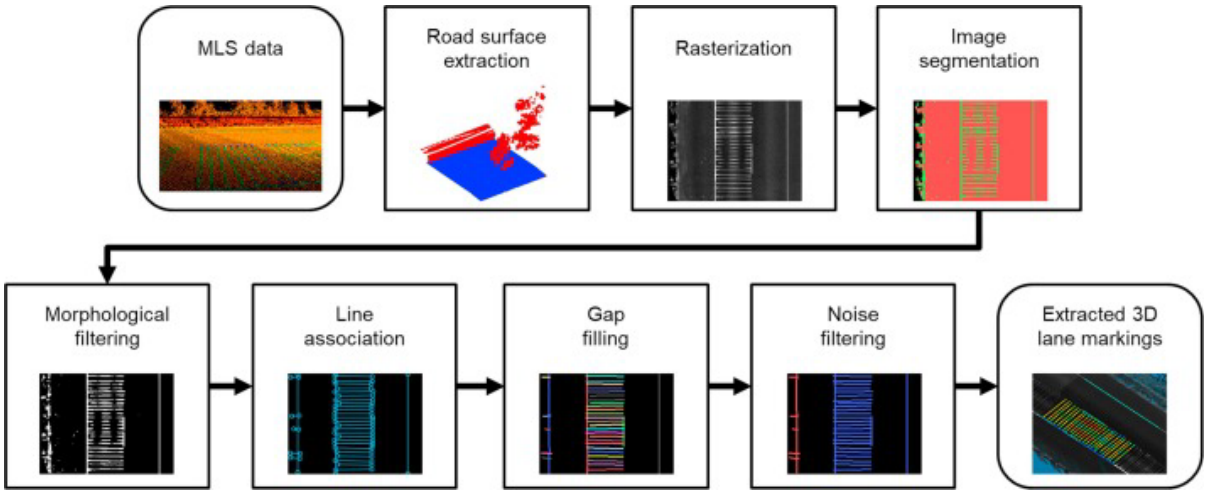

Figure 2.4: Overview of the RoME algorithm

In this study, the research team made the following revisions in the workflow of the original RoME algorithm so that it would fit the overall workflow of this project better, including (1) the modification of the algorithm to work with longitudinal markings instead of the originally proposed transversal markings; (2) the modification of linkage of markings by introducing the correspondence with the vehicle's data collection trajectory; (3) the removal of noise reduction step thanks to the efficient longitudinal marking linkage process. The revised algorithm demonstrated satisfactory performance for identifying most pavement marking-associated points. It should be noted that the processing pipeline in this research does not exclusively rely on the revised RoME algorithm. Any LiDAR-based pavement marking identification algorithms can be seamlessly embedded in the pipeline of this study.

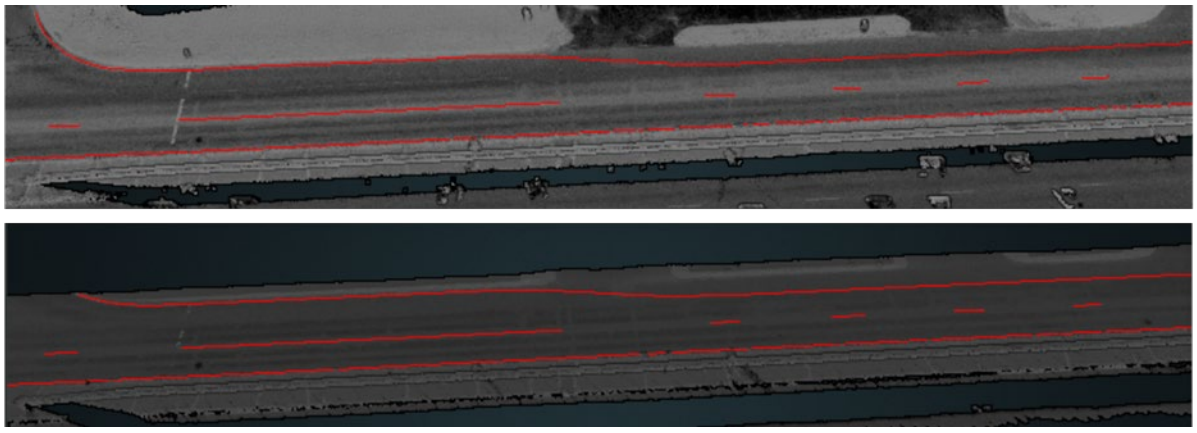

Figure 2.5: Sample results of the automated pavement extraction algorithm

2.5 Retroreflectivity Condition Evaluation

2.5.1 Correlation between LiDAR Retro-Intensity and Retroreflectivity

The retroreflectivity for pavement markings is the most critical feature for nighttime driving safety. It is defined as the luminance ratio that is redirected from the marking's surface to the illuminance originating from a vehicle's headlight *(5)*. Therefore, pavement markings of different materials consist of the reflective material (e.g., glass beads, prismatic elements, etc.) for redirecting the light from the headlight and binding material (e.g., waterborne paint, thermoplastic, etc.) for binding the reflecting material with the pavement and providing color information. A LiDAR system collects the retro-intensity values in a way similar to the measurement of pavement marking retroreflectivity. A retro-intensity value is acquired with each LiDAR point, which measures the ratio of the energy redirected from the object to the energy emitted from the LiDAR sensor. Hence, a possible correlation exists between the retro-intensity values and the pavement marking retroreflectivity conditions. Such a correlation can potentially be used to conduct an automatic pavement marking retroreflectivity condition assessment. In fact, a similar approach has been developed and validated for traffic sign retroreflectivity conditions *(49,50)*. The unique challenge for pavement marking retroreflectivity, in contrast to traffic signs, is twofold: (1) the degradation of retroreflectivity of pavement markings may be sourced from the failure of the reflective material that causes reduced reflectance or the failure of binding material that causes direct loss of the reflective material; (2) comparing with traffic signs, pavement marking has a much smaller dimension, and consequently the corresponding LiDAR point cloud has a much smaller population of measurements to evaluate the reflectance. Therefore, it is critical to re-examine the feasibility of corresponding retro-intensity values with retroreflectivity measurements for pavement marking.

This study established the initial correlation between retro-intensity values and retroreflectivity measurement between the LiDAR sensor (i.e., Riegl VMZ2000) and the StripeMaster II retroreflectometer. Figure 2.6 illustrates the principle of the handheld retroreflectometer defined in ASTM E1710-18 *(51)*, where the active window size of 6cm x 20cm was defined in the model RoadVista StripeMaster II. The retroreflectivity with the active window is averaged to obtain the retroreflectivity measurement. To ensure accurate spatial correspondence between the measurements from mobile LiDAR and the active window of the handheld retroreflectometer, all the locations for establishing the correlation were labeled. The active window was identified in the obtained LiDAR point cloud. As shown in Figure 2.7, the retro-intensities within the identified active windows were averaged (following the same specification in ASTM E1710-18).

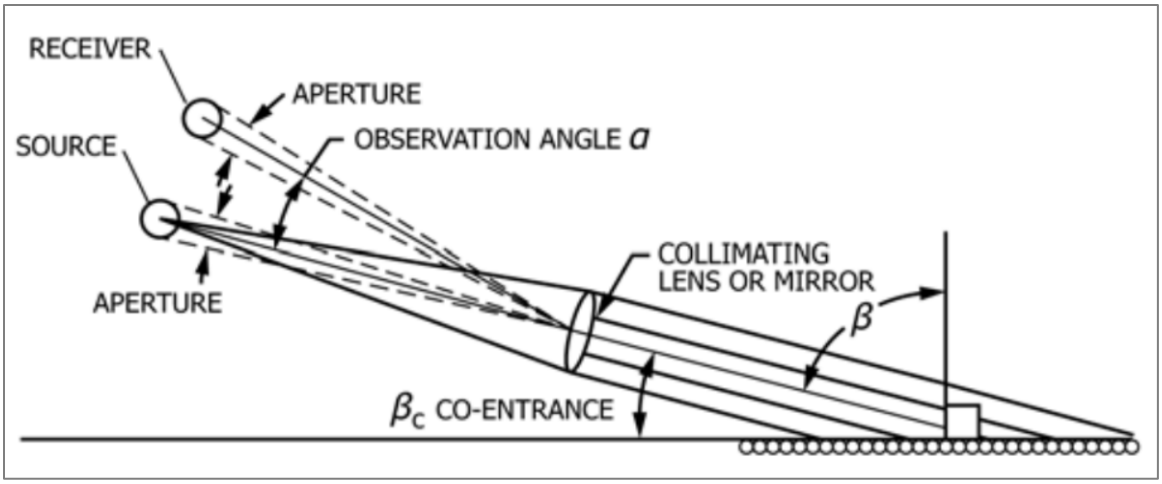

Figure 2.6: Principal of the handheld retroreflectometer measurement

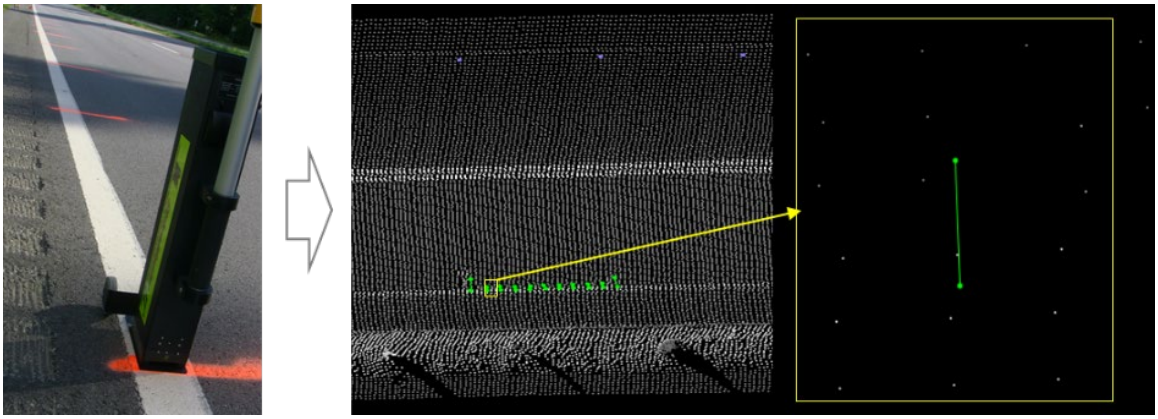

Figure 2.7: Data collection at the labeled locations using retroreflectometer and mobile LiDAR

Out of the 14 selected testing sections, the research team selected 100 samples from each section with different pavement marking materials to establish the correlation, namely thermoplastic from Sites #1, 3, 6, and 8, epoxy from Sites #4 and 7, and polyurea from the rest of the Sites. Due to the different installation dates of pavement markings in the sections, the ranges of retroreflectivity vary among different sections. The retroreflectivity values ranging between 43 and 600 mcd/m^2/lux were grouped together to establish the correlation. Figure 2.8 shows the correlation between the raw retro-intensity values from the LiDAR sensor and the retroreflectivity measurement from the handheld retroreflectometer. The result shows a clear correlation between retro-intensity and retroreflectivity. While the R-value of 0.7996 confirms a strong correlation, the scatter pattern shows a possible departure from the original assumption of a simple linear correlation. From the literature review, it is identified that similar results have been identified in previous experiments in Illinois *(52)* and Oregon *(2)*.

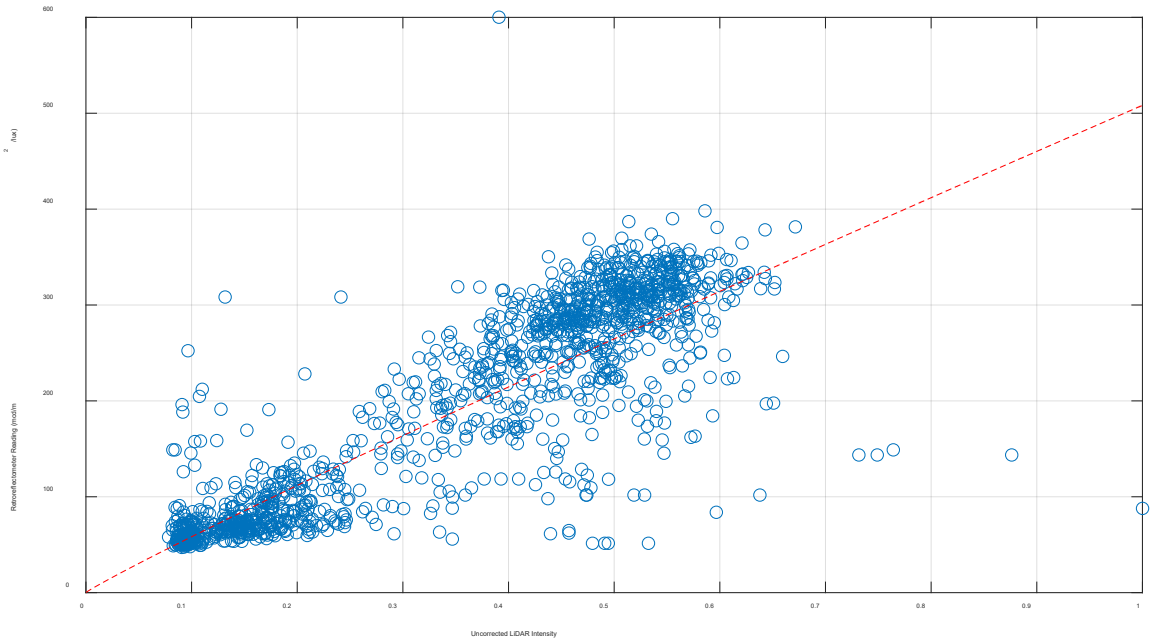

Figure 2.8: Correlation between the retro-intensity and retroreflectivity

2.5.2 LiDAR Retro-Intensity Normalization

Similar to any optic sensors, the magnitude of energy received from the targeting object for mobile LiDAR is a function of the physical property of the object surface (i.e., energy absorbing, reflecting, and diffusing capabilities), as well as a function of the transmitting distance and the incidence angles when the energy beam is intersecting with the object surface. Figure 2.9 shows an illustration of such a general model in the context of pavement markings.

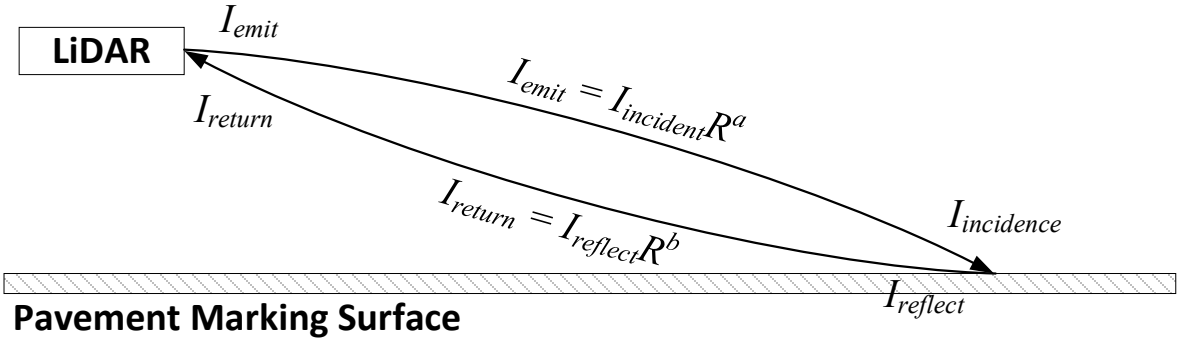

Figure 2.9: LiDAR scanning at the pavement marking surface

where R represents the distance between the LiDAR sensor and the object, i.e., the pavement marking surface, where a and b are the coefficients to be calibrated. By further incorporating the LiDAR energy models developed by Ai and Tsai *(49)*, the final form of the ratio between

the energy received (returned from the targeting object) and emitted by LiDAR can be formulated as shown in the following equation:

$$\rho = \frac{I_{return}}{I_{emit}} = \frac{I_{reflect}R^{a}}{I_{incident}R^{-b}} = [(1 - k_s(\vartheta))cos(\vartheta) + k_s(\vartheta)] \cdot R^{a+b} = f(\vartheta) \cdot g(R)$$

where k_s is the coefficients of specular reflection; ϑ is the incidence angle. It should be noted that the ambient lighting and diffused reflection, represented by k_a and k_d ($k_a + k_d + k_s = 1$), respectively, do not affect the ratio ρ *(49)*. Therefore, the effects of the beam distance (i.e., transmission distance between the mobile LiDAR and pavement marking surface) and the incidence angle (i.e., the angle of the LiDAR beam and the pavement marking surface) can be independently formulated, whereas the coefficient a, b, and k_s were to be estimated.

The same phenomenon was observed for pavement marking. While similar closed-form equation as the previous work by Ai and Tsai *(49)* may be established for pavement markings, the research team developed empirical look-up tables in this study for two reasons: 1) while the independent equations for beam distance and incidence angle were achieved by isolating parameters of $a+b$ and k_s for traffic signs through empirical modeling, it is achievable, and yet challenging for pavement marking, since only a very limited number of sample points maybe acquired for pavement markings and the ground truth (i.e., handheld retroreflectometer) is an estimate from a large footprint (i.e., 6 cm by 20 cm); 2) while the closed-form equation is ideal for computation, a look-up table is a more efficient means to batch process a large volume of sequential data, i.e., pavement markings.

Therefore, two look-up tables were established in this study. It should be noted that two different look-up tables were established based on the form of the reflecting elements, i.e., glass beads on flat surfaces and glass beams on preformed structures, instead of the actual material type. Figure 2.10(a) shows the look-up table for glass beads on flat surfaces, including materials of thermoplastics, epoxy, polyurea, waterborne paint, etc., whereas Figure 2.10(b) shows the look-up table for glass beads on structured surfaces, e.g., preformed tapes. It can be observed that the look-up table in Figure 2.10(b) shows a small dip when the incidence angle is around 50 degrees, which is introduced by diffused reflection effect by the structured surface. While such a phenomenon is critical for analyzing preformed tapes, in this study, only the look-up table in Figure 2.10(a) was used as the selected sections do not consist of any preformed tape sections.

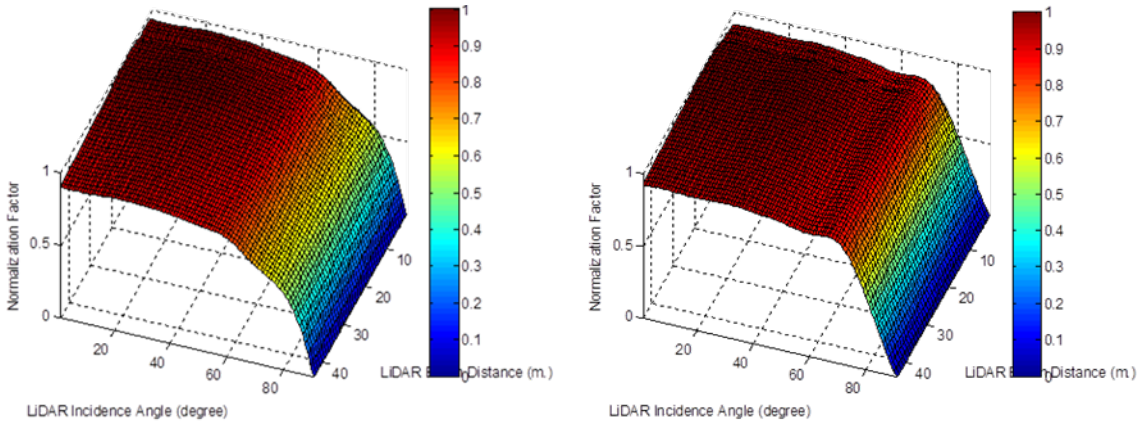

Figure 2.10: Look-up tables for range and incidence angle normalization

By applying the normalization look-up table shown in Figure 2.10(a), the correlation between the retro-intensity values from the mobile LiDAR and the retroreflectivity measurement from the handheld retroreflectometer is adjusted, as shown in Figure 2.11. The dots with dark red lines are the ones that were normalized based on their scanning beam distances and incidence angles. It can be observed that the correlation has been significantly improved with an R^2 of 0.9296. The empirical equation with coefficients of 505.0564 and 0.9717 is used for the remainder of this study.

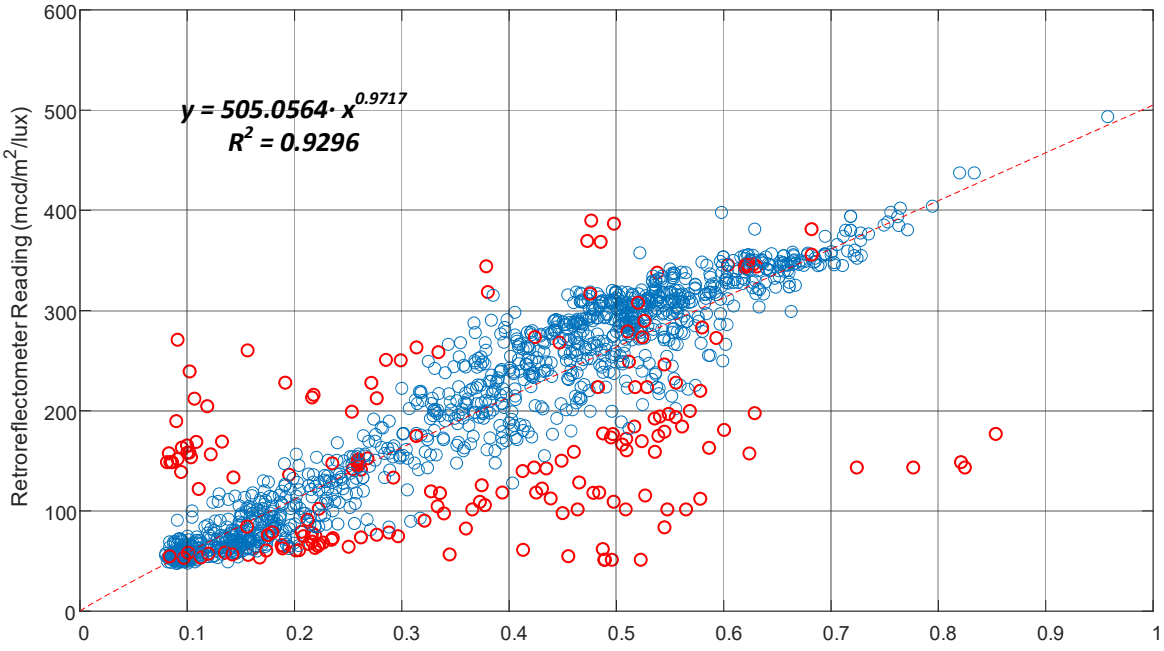

Figure 2.11: Correlation between retro-intensity and retroreflectivity after normalization

2.6 Surface Condition (Percentage Loss) Evaluation

The objective of surface condition evaluation is to determine the percentage loss of the base material for pavement markings. As discussed in Section 2.5, the loss of retroreflectivity may be attributed to two main factors, loss of reflective material and loss of base material (and consequently reflective material). In this study, the surface condition evaluation is conducted based on the image processing results and subsequently projected to the registered point cloud data.

2.6.1 Image Binarization

Pavement markings are purposely designed with distinct colors and contrast, i.e., white and yellow on dark pavements, so that their visibility can be maximized. Therefore, the task of identifying pavement marking location can be formulated as an image binarization problem, where classes 1 and 0 represent pavement marking-associated pixels (i.e., bright pixels) and non-pavement-marking-associated pixels (i.e., dark pixels).

In this study, Otsu's method *(53)* was introduced to binarize the image. It should be noted that other pavement marking extraction methods, as presented in the literature review, can also take the place of Otsu's method. In addition, there is a distinction between the pavement marking extraction method using point cloud data, presented in Section 2.4, and the algorithm presented in this subsection. The results for the pavement marking extraction using point cloud data are polylines that represent the linearly referenced locations of pavement markings for inventory retroreflectivity evaluation (i.e., identifying the active windows of LiDAR points), whereas the results from this subsection using images are regions (polygons) that present the identifiable regions of pavement markings for percentage loss analysis (i.e., identifying the pavement marking-associated pixels). It should be noted that the image binarization process presented in this subsection leveraged the extracted pavement marking location and the image-LiDAR projection that is presented in Section 2.6.2.

The principle of Otsu's method is to exhaustively search for the threshold that will minimize the variance within each class of the binarization. The objective function of the optimization is defined as the weighted sum of variances of the two classes:

$$\sigma_w^2(t) = \omega_0(t)\sigma_0^2(t) + \omega_1(t)\sigma_1^2(t)$$

where weights ω_0 and ω_1 are the probabilities of the two classes binarized by the threshold *t*, and σ_0^2 and σ_1^2 are the variances of the two classes. To compute the weights for each of the classes (i.e., pavement marking pixels and non-pavement-marking pixels), all the possible thresholds t were evaluated to identify the best threshold that maximizes σ_w^2. Figure 2.12

shows the results of the image binarization with different percentages of material loss. In the subsequent steps, the binarization results will be projected from the image coordinates to the 3D Cartesian coordinate system so that the percentage of material loss can be estimated.

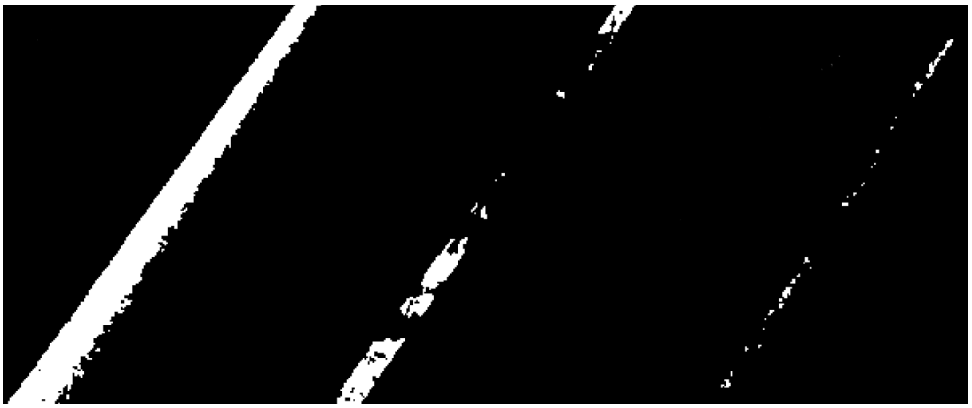

Figure 2.12: Sample binarization results with different percentages of material loss

2.6.2 Image Projection

The objective of image projection is to obtain the transformation matrix between the image coordinate system and the LiDAR sensor. The GPS coordinates embedded in each LiDAR point are transformed into local Cartesian coordinates *(49)*, e.g., North-East-Down (NED) system. Using the collinear relationship, each point in the local Cartesian coordinates can be mapped with the image coordinate system. Hence, the entire LiDAR point cloud will be colorized by the image intensity. In this case, the LiDAR point cloud will be colorized with the binarization results (i.e., Class 0 as non-pavement marking and Class 1 as pavement marking). The sensor configuration information will be input into the transformation, including the bore-sight angle of the LiDAR and the camera, the translations among the LiDAR, the camera, and the inertial navigation systems (INS). As presented in Section 2.3, the mobile LiDAR used in this study has registered with the video logging system. Therefore, the transformation matrix has been internally determined using sensor-dependent tools. In addition, the research team also developed a generalized tool for this image projection step so that LiDAR and video log imagery data collected by other sensors can also be tightly registered and take advantage of the developed methodology in this study.

2.6.3 Percentage of Material Loss Estimation

With the identified and projected regions for pavement markings, the percentage of pavement material can be estimated based on the ratio of the area for the pavement marking area (i.e., Class 1) and the bounding box area (i.e., Classes 0 and 1), as shown in the following equation:

$$\%\ of\ material\ loss = 1 - \frac{Pavement\ Marking\ Area\ (Class\ 1)}{Bounding\ Box\ Area\ (Class\ 0 + Class\ 1)}$$

where the total number of projected Class 1 pixels is used to estimate the pavement marking area, and the total number of pixels in the minimum-area rectangle is used to estimate the areas for Class 0 (i.e., area with material loss) and Class 1 (i.e., area without material loss). Figure 2.13 shows the results of the 5% material loss and 45% material loss at the same road section (2020 and 2021, respectively).

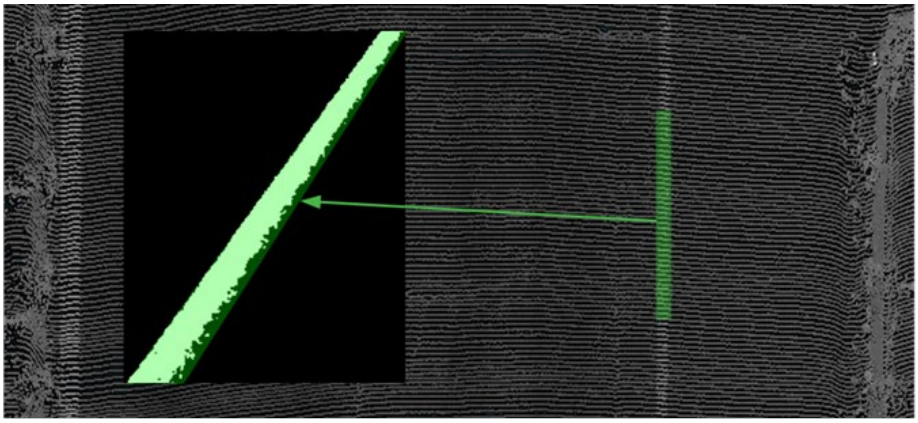

(a)

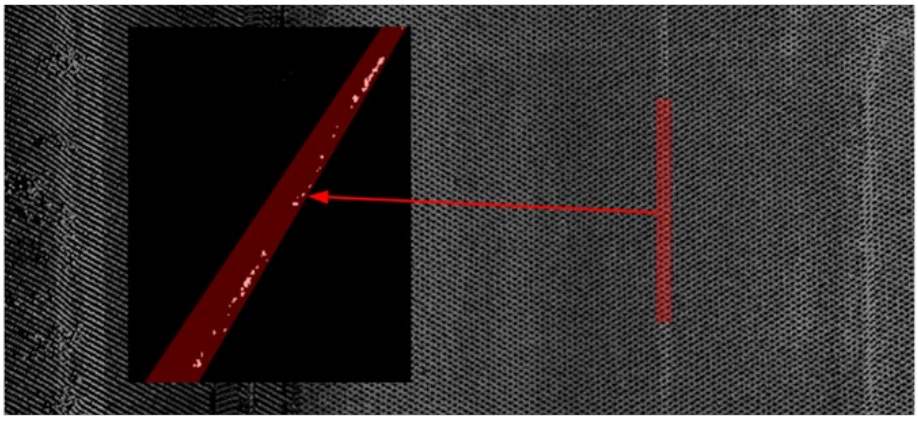

(b)

Figure 2.13: Same road section with material losses of 5% and 45%

3.0 Results

The results of this study are presented to answer three fundamental questions for pavement marking management, including (1) whether the mobile LiDAR-based method is a feasible means for inventorying pavement markings and evaluating their corresponding condition; (2) whether different pavement marking materials behave differently in their retroreflectivity performance; (3) what the effect does surface material loss have on the overall retroreflectivity condition. Subsections 3.1, 3.2, and 3.3 present the corresponding findings for these three fundamental questions.

3.1 Pavement Marking Inventory

In this study, mobile LiDAR and video log imagery data were collected along the selected 14 representative testing sections covering different roadway classifications and pavement marking materials, covering three timestamps six months apart. Using the developed pavement marking extraction algorithm, the retroreflectivity condition evaluation method (with normalization), and the surface percentage loss estimation method, a complete inventory geodatabase, containing all the pavement property and condition information, was derived. Figure 3.1 shows the overview of the 14 testing sections and the corresponding results. For example, for Site #14 along State Route 9 east bound near, the average retroreflectivity condition is 175 mcd/m^2/lux, and the average loss of material is approximately 14%.

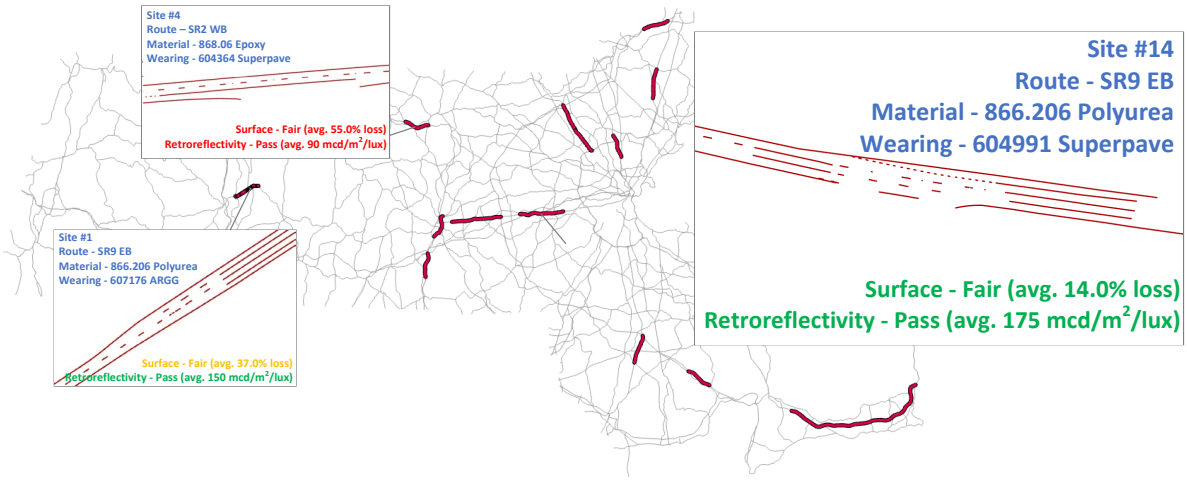

Figure 3.1: Overview of the 14 selected testing sections

In this study, the retroreflectivity condition and the loss of material can be estimated at different intervals thanks to the continuous measurements from mobile LiDAR and video log

images. To make a consistent reporting interval (e.g., mobile retroreflectometer), the continuous measurements were aggregated based on a 100 ft. interval and then reported to the geodatabase for pavement marking inventory. A separate database storing all the raw, continuous measurements for retroreflectivity and loss of material was also created and referenced to each of the 100 ft. sections.

3.2 Retroreflectivity Condition Evaluation

3.2.1 Retroreflectivity Repeatability and Accuracy

The objective of this experimental test is to assess the feasibility of the developed LiDAR-based retroreflectivity condition evaluation method. The feasibility is evaluated from two perspectives, including the repeatability and the accuracy of the condition evaluation.

- *Repeatability*: The repeatability of the method represents the consistency of the measurements with the same material and under the same data collection condition. The repeatability of a measurement method is a foundational requirement for producing reliable and consistent results, especially for temporal analysis. Therefore, the research team evaluated different data collection runs along the testing sections with different marking materials, different ranges of retroreflectivity values, and different levels of ambient lighting conditions. The results show that the LiDAR-derived retroreflectivity maintains consistent repeatability. Figure 3.2 shows an example of the repeatability results from a sample section along testing Site #4. Figure 3.2(a) shows that the retroreflectivity measurements along different runs show almost identify resemblance, which indicates desirable repeatability, although the data collection for Run1 and Run2 were conducted at separate times of the day and at different driving speeds. Figure 3.2(b) shows the quantitative measure of the repeatability by correlating the measurement between Run 1 and Run 2 and clearly demonstrates the excellent repeatability of the developed LiDAR-based method.
- *Accuracy*: The accuracy of the method represents how close the measurement from mobile LiDAR is to the ground truth. For LiDAR-based pavement marking retroreflectivity measurement, due to the dynamic nature of the data collection, it is challenging to make a fair comparison with any "ground truth." In this study, the research team selected RoadVista LaserLux mobile retroreflectometer as the baseline for comparison, as it is an approved method and system by ASTM for pavement marking retroreflectivity measurement. Figure 3.3 shows a picture of the staging RoadVista LaserLux system and the mobile LiDAR system right before the data collection.

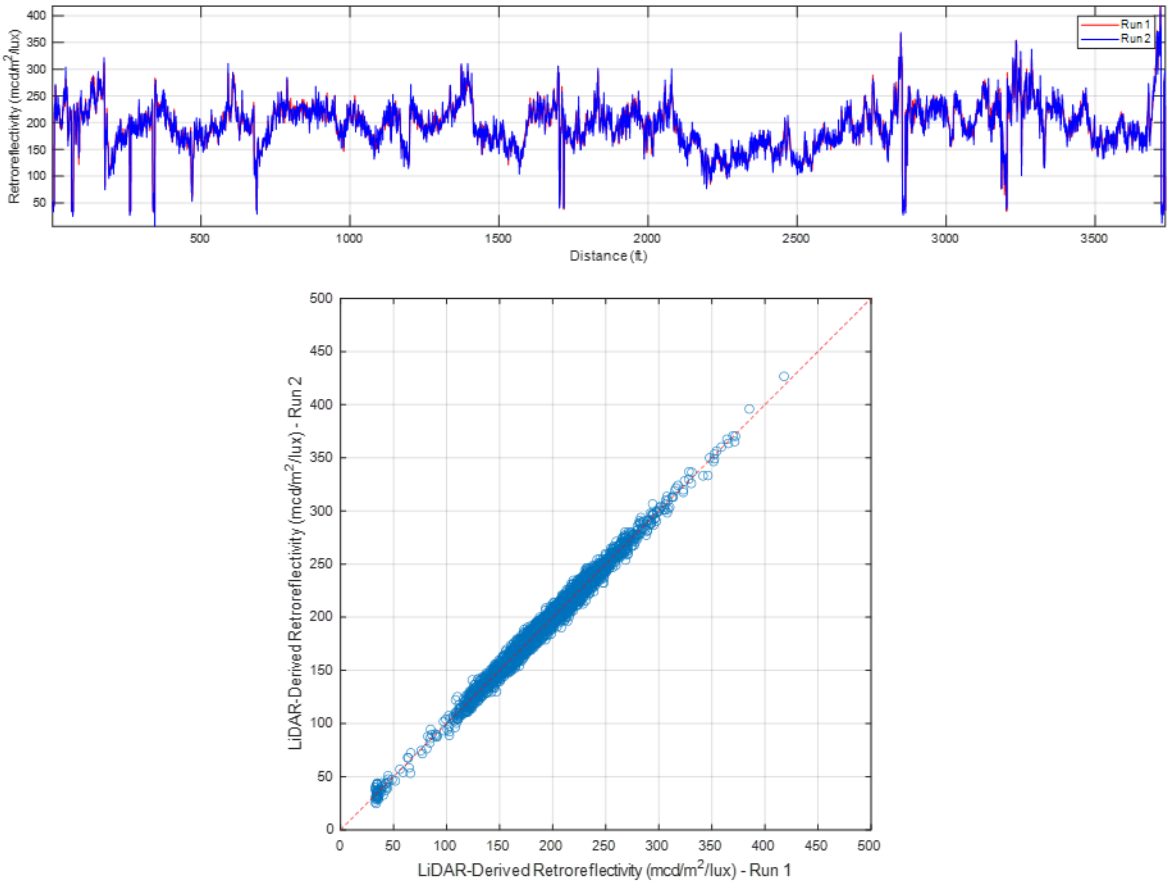

Figure 3.2: Repeatability result using the developed LiDAR-based method

Figure 3.3: Staging phase of the RoadVista LaserLux and the Riegl VMZ2000 systems

The data collected from these two systems was conducted along the same section of the road with the same starting and ending points. As the LaserLux system aggregates and reports retroreflectivity measurements at the interval of 0.01 miles, the continuous measurements from the mobile LiDAR system were also aggregated to the same interval for comparison. Figure 3.4 shows an example of the comparison between the mobile retroreflectometer measurements and the aggregated LiDAR-derived retroreflectivity along Site #9, which shows consistent results along the entire road section regardless of the actual condition of the pavement markings. Similar tests were conducted in the rest of the testing sections, and the correlations between the two methods all display a similar resemblance, as shown in Figure 3.4(b). Although most of the scattered points were evenly and tightly distributed along the diagonal direction, which indicates a good correlation, it can be observed that some of the measurements farther depart from the diagonal line. These outliers may be attributed to the mismatch of the locations where measurements were conducted by the two methods.

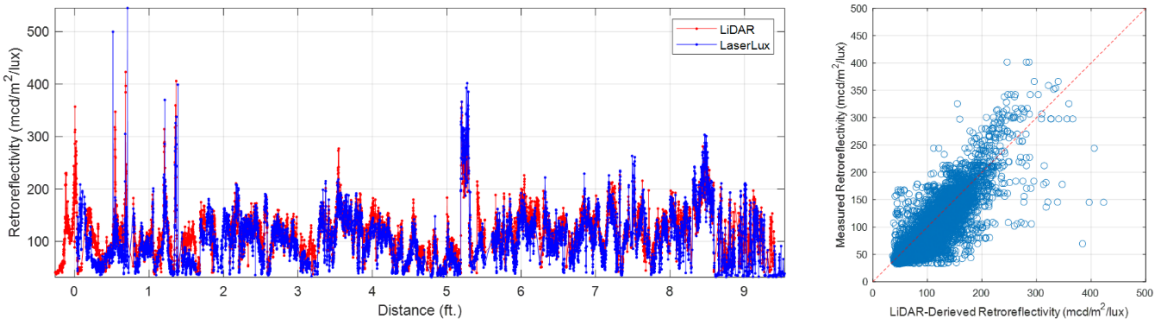

(a) **(b)**

Figure 3.4: Correlation between retroreflectometer measurements and LiDAR-derived retroreflectivity

3.2.2 Retroreflectivity Deterioration

One of the main objectives of this study is to investigate the feasibility of the LiDAR-based retroreflectivity condition evaluation method for identifying temporal retroreflectivity condition deterioration. In this study, three types of materials were studied along the 14 selected testing sites, including polyurea, epoxy, and thermoplastics.

- *Polyurea*: There are eight testing sections that include polyurea pavement marking, with installation years between 2012 and 2021. Figure 3.5 shows an example results along testing Site #13 on US6. The results show that, at comparable annual average daily traffic (AADT) levels, the deterioration rate for polyurea material is consistently less than 10 mcd/m^2/lux annually. In addition, the deterioration variability along all the sections is around 2 mcd/m^2/lux. Similar observations were identified in other polyurea testing sections in this study. These observations imply that, regardless of the installation year,

the current retroreflectivity, or the location of the sections, the deterioration of retroreflectivity for the polyurea material is slow (i.e., <10 mcd/m^2/lux) and consistent throughout the entire section (i.e., ~2 mcd/m^2/lux).

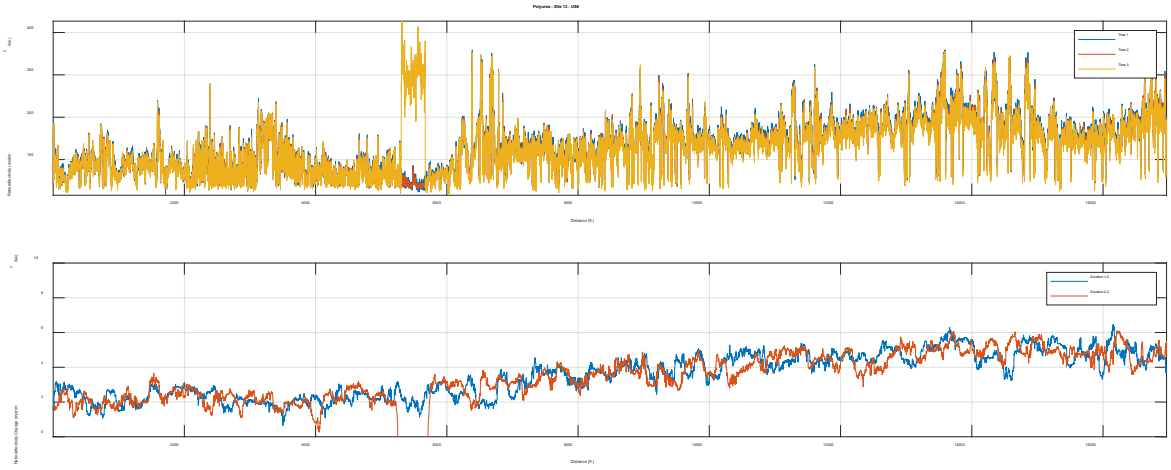

Figure 3.5: Retroreflectivity deterioration results for polyurea Site #13

- *Epoxy*: There are two testing sections that include epoxy pavement marking, with installation years between 2011 and 2022. Figure 3.6 shows an example results along testing Site #7 on I-93. The results show that, even after 10 years since installation, the deterioration rate for epoxy material is around 10 mcd/m^2/lux annually. In addition, the deterioration variability along all the sections is between 3 and 5 mcd/m^2/lux. Similar observations were identified in the other epoxy testing section in this study. These observations imply that, regardless of the current retroreflectivity or the location of the sections, the deterioration of retroreflectivity for the epoxy material is relatively slow (i.e., ~10 mcd/m^2/lux) and consistent throughout the entire section (i.e., 3–5 mcd/m^2/lux).

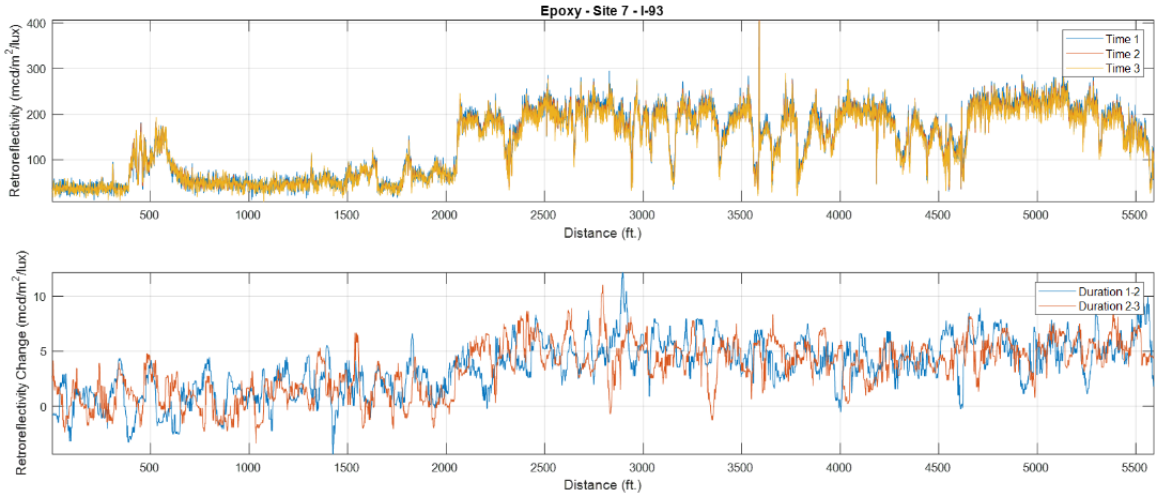

Figure 3.6: Retroreflectivity deterioration results for epoxy Site #7

- *Thermoplastic*: There are four testing sections that include thermoplastic pavement marking, with installation years between 2005 and 2022. Figure 3.7 shows an example results along testing Site #1 on SR9. The results show that, at comparable AADT levels, the deterioration rate for thermoplastic material is 20–30 mcd/m^2/lux annually. In addition, the deterioration variability along all the sections is between 10–15 mcd/m^2/lux. Similar observations were identified in the other thermoplastic testing section in this study. These observations imply that, regardless of the current retroreflectivity or the location of the sections, the deterioration of retroreflectivity for the thermoplastic material can be fast (i.e., 20–30 mcd/m^2/lux) and may vary significantly along the same section (i.e., 10–15 mcd/m^2/lux).

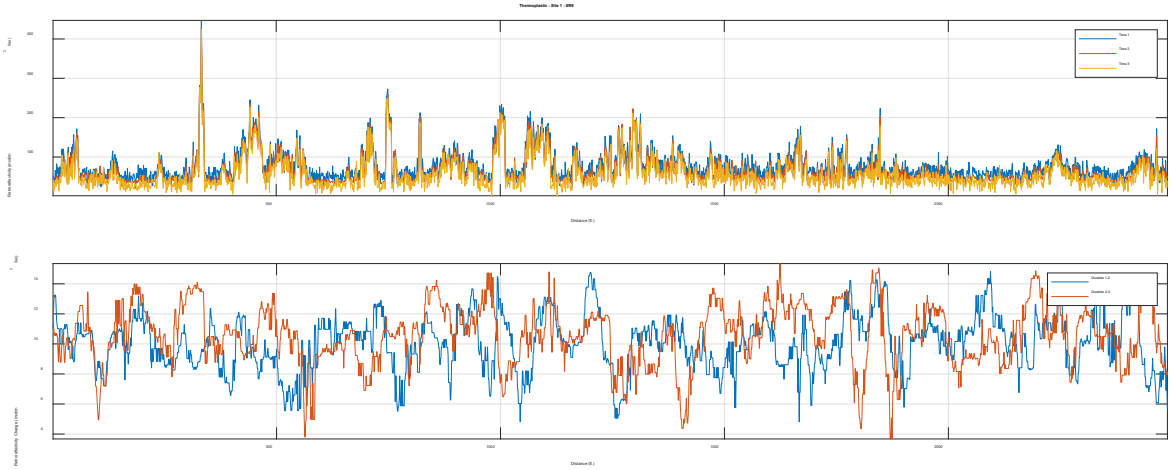

Figure 3.7: Retroreflectivity deterioration results for thermoplastic Site #1

3.3 Effect of Surface Condition on Retroreflectivity

Through the observations of three different pavement marking materials, it should be noted that the deterioration trends (rate and variability) of retroreflectivity vary by material, but do not vary by the installation year, the current retroreflectivity, or the number of days from installation. However, the material of thermoplastic shows much larger deterioration rates and variability along the same section for all of the four thermoplastic sections. A further investigation on the effect of material loss on retroreflectivity was conducted on the thermoplastic sites, where large variability of deterioration was observed. Figure 3.8 shows the change of retroreflectivity observed along Site #1 between August 2020 and August 2021. It can be noted that two significant phenomena, including (1) the change of retroreflectivity is around 20 mcd/m^2/lux, which is quite large within the a-year window; (2)

the variability of the change within the same section can be as high as 8 mcd/m^2/lux. A further investigation at the locations where substantial changes of retroreflectivity were observed, e.g., the location highlighted in Figure 3.8, revealed that the change may be attributed to the significant amount of material loss (due to the weak binding of thermoplastic material).

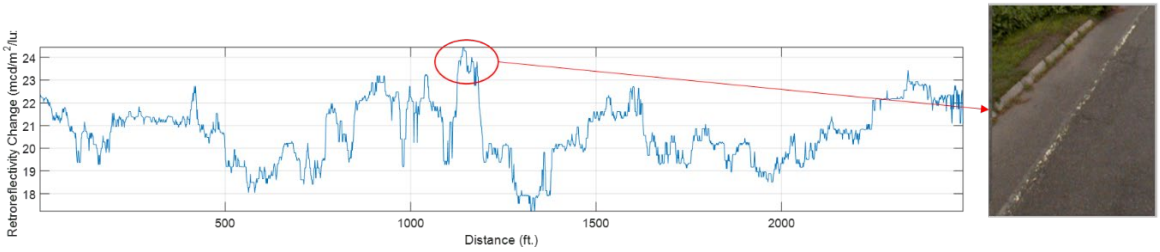

Figure 3.8: Retroreflectivity deterioration (difference between 2020 and 2021) along Site #1 and the corresponding binding material loss

Therefore, the research team further investigated the relationship between the change of surface material percentage loss and the annual change of retroreflectivity and the relations hip between the surface material percentage loss and the current retroreflectivity. Figure 3.9 shows the results of these exploratory correlations. Figure 3.9(a) shows that the change of surface material loss is linearly correlated to the annual change of retroreflectivity. It indicates that instead of the deterioration of the reflective beads, the loss of the material (with the embedded beads) was the primary contributor to the deterioration of retroreflectivity. In contrast, Figure 3.9(b) shows that the change in surface material loss does not dictate the current retroreflectivity condition. It indicates that a higher level of material loss does not imply a lower retroreflectivity as long as the reflective beams embedded in the remaining binding material remain reflective and that a lower level of material loss does not imply a better reservation of retroreflectivity if the reflective beams embedded in the binding material has already deteriorated.

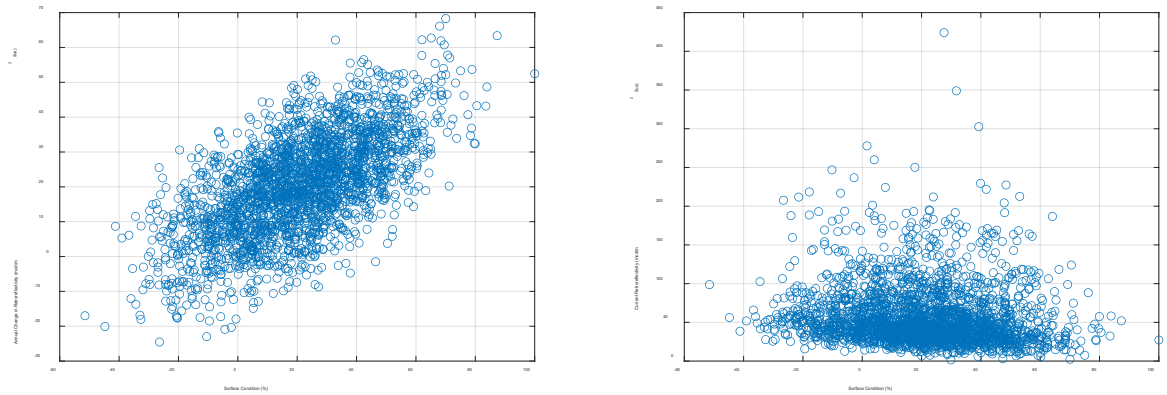

(a) **(b)**

Figure 3.9: Exploratory correlations between retroreflectivity and the loss of material

This page left blank intentionally.

4.0 Conclusions

This study is aimed at utilizing mobile LiDAR and video log imagery data and developing an automated method for the extraction, localization, and retroreflectivity condition assessment of in-service pavement markings. The research team selected 14 representative testing sections with various road characteristics, pavement marking materials, and installation times, were selected and analyzed within this study. The detailed objectives include:

- Develop and validate an automated method for the inventory and retroreflectivity condition assessment for pavement markings as a proof of concept by leveraging the mobile LiDAR and video log images.
- Investigate the feasibility of identifying deterioration trends of retroreflectivity conditions using the developed LiDAR-based method for better defining the benefit-to-cost ratio of different pavement marking materials in the future and eventually leading toward the MassDOT's pavement marking standards.

The deliverables of this study include a complete, georeferenced pavement marking inventory with retroreflectivity condition measurements for the 14 selected road sections. The georeferenced inventory database also includes the retroreflectivity deterioration trends covering three observation timestamps (i.e., 6-month intervals) within the duration of this study.

The outcome of this study is summarized as follows:

- *A Review of Pavement Marking Efforts*. The research team conducted a detailed literature review of available and ongoing research through TRID on pavement marking inventory and condition evaluation methods and mobile LiDAR applications in pavement marking studies.
- *Mobile LiDAR Data Acquisition*. The research team conducted a comprehensive data acquisition and data preprocessing using the mobile LiDAR sensor (i.e., Riegl VMZ-2000) along with the 14 selected testing sections. The LiDAR data collected in 2016 by MassDOT was also incorporated into the final dataset.
    - The collected data cover more than 70 miles of different classifications of highways, with different pavement marking material types.
    - For each testing section, three data collections were conducted at a 6-month interval to monitor the deterioration of the pavement markings.
    - Addition data collection with mobile LiDAR, handheld retroreflectometer, and mobile retroreflectometer was conducted at the beginning of the study for the method development and result validation.

- *Automated Pavement Marking Extraction*. The research team developed an automated pavement marking extraction algorithm based on the existing effort by the Oregon Department of Transportation and Oregon State University using RoME. The new automated pavement marking extraction was customized to fit the workflow of this study, including the longitudinal line extraction, break line linkage, and noise reduction. The developed algorithm is used to identify the delineations of the pavement markings in the 14 testing sections and establish the spatial references in the final inventory database.
- *Automated Pavement Marking Retroreflectivity Condition Evaluation*. The research team developed an automated pavement marking retroreflectivity condition evaluation method through the correlation between the retro-intensity from mobile LiDAR and the retroreflectivity measurements from handheld/mobile retroreflectometer. A customized normalization scheme was created to rectify the retro-intensity measurements based on the distance and incidence angle of the LiDAR scanning beam.
    - The research team validated the repeatability and accuracy of the developed method. The results demonstrated a close correlation with the mobile retroreflectometer and superior repeatability over the mobile retroreflectometer. The disparity between the developed method and the mobile retroreflectometer measurements was attributed to the mismatch of locations from both methods.
    - The research team incorporated the surface material loss into the pavement marking inventory results. The material loss is not only an important condition indicator for pavement markings; it is identified that the percentage loss also played an important role in determining retroreflectivity conditions, especially for materials that may experience binding failure due to age and fatigue.
- *Pavement Marking Retroreflectivity Condition Deterioration*. The research team utilized the developed automated algorithms and methods and investigated the deterioration trends for the three pavement marking materials in the selected testing sections, including polyurea, epoxy, and thermoplastic. With three 6-month observation windows, initial deterioration trends were established, and the difference in materials was investigated.
    - At comparable AADT levels, deterioration rates varied among three tested materials: (1) polyurea has a minimum annual deterioration of less than 10 $mcd/m^2/lux$; (2) epoxy has a consistent annual deterioration of around 10 $mcd/m^2/lux$; (3) thermoplastic has a much larger deterioration of 20–30 $mcd/m^2/lux$.
    - Regardless of the installation locations and years, deterioration variability was observed differently for the three tested materials: (1) polyurea and epoxy have a small deterioration variability along the same testing section at less than 5 $mcd/m^2/lux$; (2) thermoplastic material has much larger variability among the same testing section at 10-15 $mcd/m^2/lux$. While the variability may be attributed

to other factors like installation inhomogeneity, a further investigation of the surface percentage loss revealed that the variability of retroreflectivity change can be attributed to the loss of binding material instead of the loss of reflective material.

- *Pavement Marking Management using LiDAR*. The research team has developed a complete methodology for automatically inventorying the location of the in-service pavement markings and evaluating their corresponding retroreflectivity condition and binding material loss, leveraging mobile LiDAR and video log imagery data. While further analysis is recommended for waterborne and preformed tape material, recessed marking, and raised pavement markers (RPMs), the outcomes of this study have demonstrated that the mobile LiDAR-based method is a feasible and reliable option for state transportation agencies to implement in their pavement marking inventory and retroreflectivity condition evaluation program.

The scope of the next phase of this study includes the following:

- To apply the developed retroreflectivity model with more frequent scanning intervals for validating some of the existing pavement marking deterioration models in previous studies using LiDAR-based retroreflectivity measurements.
- To apply the developed methodology in a larger network for establishing a comprehensive pavement marking inventory on a network level and for further validating the feasibility of the methodology for other materials (i.e., waterborne and preformed tape), different installation technologies (i.e., recessed marking, wet performance marking, RPMs, etc.).
- To develop a pavement marking management program based on the developed LiDAR-based methodology, including the assessment of both in-service and newly installed pavement markings.

This page left blank intentionally.

5.0 References

1. FHWA. Nighttime Visibility - Safety. FHWA, Washington, D.C., 2020. Accessed August 18, 2020. https://safety.fhwa.dot.gov/roadway_dept/night_visib/general-information.cfm.
2. Olsen, M. J., C. E. Parrish, E. Che, J. Jung, and J. Greenwood. LIDAR for Maintenance of Pavement Reflective Markings and Retroreflective Signs: Vol. I Reflective Pavement Markings. Final Report. Oregon Department of Transportation, Salem, OR, 2018.
3. Pike, A., and T. Barrette. Pavement Markings—Wet Retroreflectivity Standards. 100. Minnesota DOT, St. Paul, MN, 2020.
4. van Schalkwyk, I. Enhancements to Pavement Marking Testing Procedures. 136. Oregon Department of Transportation, Salem, OR, 2010.
5. FHWA. Manual on Uniform Traffic Control Devices for Streets and Highways. FHWA, Washington, D.C., 2009.
6. Schaepman-Strub, G., M. E. Schaepman, T. H. Painter, S. Dangel, and J. V. Martonchik. Reflectance Quantities in Optical Remote Sensing—Definitions and Case Studies. *Remote Sensing of Environment*, Vol. 103, No. 1, 2006, pp. 27–42. https://doi.org/10.1016/j.rse.2006.03.002.
7. Lloyd, J. n.d. A Brief History of Retroreflective Sign Face Sheet Materials.
8. Burns, D. M., T. P. Hedblom, and T. W. Miller. Modern Pavement Marking Systems: The Relationship Between Optics and Nighttime Visibility. *In Transportation Research Record: Journal of the Transportation Research Board*, No. 2056, Transportation Research Board of the National Academies, Washington, D.C., 2008, pp. 43–51.
9. Migletz, J., J. L. Graham, K. M. Bauer, and D. W. Harwood. Field Surveys of Pavement-Marking Retroreflectivity. *In Transportation Research Record: Journal of the Transportation Research Board*, No. 1657, Transportation Research Board of the National Academies, Washington, D.C., 1999.
10. Schnell, T., F. Aktan, and Y.-C. Lee. Nighttime Visibility and Retroreflectance of Pavement Markings in Dry, Wet, and Rainy Conditions. *In Transportation Research Record: Journal of the Transportation Research Board*, No. 1824, Transportation Research Board of the National Academies, Washington, D.C., 2003.
11. Lundkvist, S.-O., and U. Isacsson. Prediction of Road Marking Performance. Journal of Transportation Engineering, Vol. 133, No. 6, 2007, pp. 341–346. https://doi.org/10.1061/(ASCE)0733-947X(2007)133:6(341).
12. Carlson, P. J., J. D. Miles, and A. M. Pike. Evaluation of Wet-Weather and Contrast Pavement Marking Applications: Final Report. Texas Department of Transportation, Austin, TX, 2007, p. 158.
13. Pike, A. M., G. Hawkins, and P. J. Carlson. Evaluating the Retroreflectivity of Pavement Marking Materials under Continuous Wetting Conditions. *In Transportation Research Record: Journal of the Transportation Research Board*, No. 2015, Transportation Research Board of the National Academies, Washington, D.C.,2007.

14. Kirk, A. R., E. A. Hunt, and E. W. Brooks. Factors Affecting Sign Retroreflectivity. 29. Oregon Department of Transportation, Salem, OR, 2001.
15. Debaillon, C., P. Carlton, Y. He, T. Schnell, and F. Aktan. Updates to Research on Recommended Minimum Levels for Pavement Marking Retroreflectivity to Meet Driver Night Visibility Needs. 46. FHWA, McLean, VA, 2007.
16. Hawkins, Jr., H. G., M. P. Pratt, and P. J. Carlson. Preliminary Economic Impacts of Implementing Minimum Levels of Pavement Marking Retroreflectivity. FHWA, Washington, D.C, 2008.
17. FHWA. National Standards for Traffic Control Devices; The Manual on Uniform Traffic Control Devices for Streets and Highways; Maintaining Pavement Marking Retroreflectivity. FHWA, Washington, D.C., 2010.
18. ASTM. WK3833 New Test Method for Determination of the Coefficient of Retroreflection of Pavement Markings Using a 30 m Geometry Mobile Retroreflectometer. ASTM WK3833, ASTM, West Conshohocken, PA, 2020. Accessed August 18, 2020. https://www.astm.org/DATABASE.CART/WORKITEMS/WK3833.htm.
19. Nolan, J., R. Eckels, M. Evers, R. Singh, and M. J. Olsen. 2015. Multi-Pass Approach for Mobile Terrestrial Laser Scanning. *ISPRS Ann. Photogramm. Remote Sens. Spatial Inf. Sci.*, Vol. II-3/W5, 2015, pp. 105–112. https://doi.org/10.5194/isprsannals-II-3-W5-105-2015.
20. Höfle, B., and N. Pfeifer. Correction of laser Scanning Intensity Data: Data and Model-Driven Approaches. *ISPRS Journal of Photogrammetry and Remote Sensing*, Vol. 62, No. 6, 2007, pp. 415–433. https://doi.org/10.1016/j.isprsjprs.2007.05.008.
21. Wagner, W. Radiometric Calibration of Small-Footprint Full-Waveform Airborne Laser Scanner Measurements: Basic Physical Concepts. *ISPRS Journal of Photogrammetry and Remote Sensing*, ISPRS Centenary Celebration Issue, Vol. 65, No. 6, 2010, pp. 505–513. https://doi.org/10.1016/j.isprsjprs.2010.06.007.
22. Kaasalainen, S., A. Jaakkola, M. Kaasalainen, A. Krooks, and A. Kukko. Analysis of Incidence Angle and Distance Effects on Terrestrial Laser Scanner Intensity: Search for Correction Methods. *Remote Sensing*, Vol. 3, No. 10, 2011, pp. 2207–2221. https://doi.org/10.3390/rs3102207.
23. Jutzi, B., and H. Gross. n.d. Normalization of LIDAR Intensity Data Based on Range and Surface Incidence Angle. 7.
24. Vain, A., S. Kaasalainen, U. Pyysalo, A. Krooks, and P. Litkey. Use of Naturally Available Reference Targets to Calibrate Airborne Laser Scanning Intensity Data. *Sensors (Basel)*, Vol. 9, No. 4, 2009, pp. 2780–2796. https://doi.org/10.3390/s90402780.
25. Kashani, A. G., M. J. Olsen, C. E. Parrish, and N. Wilson. A Review of LIDAR Radiometric Processing: From Ad Hoc Intensity Correction to Rigorous Radiometric Calibration. *Sensors*, Vol. 15, No. 11, 2015, pp. 28099–28128. https://doi.org/10.3390/s151128099.

26. Jelalian, A. V. Laser Radar Systems. Artech House, Boston, 1992.
27. Baltsavias, E. P. Airborne Laser Scanning: Basic Relations and Formulas. *ISPRS Journal of Photogrammetry and Remote Sensing*, Vol. 54. No. 2, 1999, pp. 199–214. https://doi.org/10.1016/S0924-2716(99)00015-5.
28. Mallet, C., and F. Bretar. Full-Waveform Topographic LIDAR: State-of-the-Art. *ISPRS Journal of Photogrammetry and Remote Sensing*, Vol. 64, No. 1, 2009, pp. 1–16. https://doi.org/10.1016/j.isprsjprs.2008.09.007.
29. Guan, H., J. Li, S. Cao, and Y. Yu. Use of Mobile LiDAR in Road Information Inventory: A Review. *International Journal of Image and Data Fusion*, Vol. 7, No. 3, 2016, pp. 219–242. https://doi.org/10.1080/19479832.2016.1188860.
30. Yang, B., L. Fang, Q. Li, and J. Li. Automated Extraction of Road Markings from Mobile Lidar Point Clouds. *Photogrammetric Engineering and Remote Sensing*, Vol. 78, No. 4, 2012, pp. 331–338. https://doi.org/10.14358/PERS.78.4.331.
31. Riveiro, B., H. González-Jorge, J. Martínez-Sánchez, L. Díaz-Vilariño, and P. Arias. Automatic Detection of Zebra Crossings from Mobile LiDAR Data. *Optics & Laser Technology*, Vol. 70, 2015, pp. 63–70. https://doi.org/10.1016/j.optlastec.2015.01.011.
32. Guo, J., M.-J. Tsai, and J.-Y. Han. Automatic Reconstruction of Road Surface Features by Using Terrestrial Mobile LIDAR. *Automation in Construction*, Vol. 58, 2015, pp. 165–175. https://doi.org/10.1016/j.autcon.2015.07.017.
33. Yao, Y. and Hu, Q. 2014. Automatic Extraction Method Study of Road Marking Lines Based on Projection of Point Clouds. *In 2014 22nd International Conference on Geoinformatics*, 1–4.
34. Smadja, L., J. Ninot, and T. Gavrilovic. Road Extraction and Environment Interpretation from LIDAR *Sensors*. 6, 2010.
35. Toth, C., E. Paska, and D. Brzezinska. Using Road Pavement Markings as Good Control for LIDAR Data. 37, 2008.
36. Zhang, H., J. Li, M. Cheng, and C. Wang. Rapid Inspection of Pavement Markings Using Mobile LIDAR Point Clouds. *International Archives of the Photogrammetry, Remote Sensing and Spatial Information Sciences*, Vol. XLI-B1, 2016, pp. 717–723. https://doi.org/10.5194/isprsarchives-XLI-B1-717-2016.
37. Vosselman, G. n.d. Advanced Point Cloud Processing. 28.
38. Yan, L., H. Liu, J. Tan, Z. Li, H. Xie, and C. Chen. Scan Line Based Road Marking Extraction from Mobile LiDAR Point Clouds. *Sensors (Basel)*, Vol. 16, No. 6, 2016, 903. https://doi.org/10.3390/s16060903.
39. Jaakkola, A., J. Hyyppä, H. Hyyppä, and A. Kukko. Retrieval Algorithms for Road Surface Modelling Using Laser-Based Mobile Mapping, *Sensors*, Vol. 8, No. 9, 2008, pp. 5238–5249. Molecular Diversity Preservation International. https://doi.org/10.3390/s8095238.
40. Guan, H., J. Li, Y. Yu, M. Chapman, and C. Wang. Automated Road Information Extraction from Mobile Laser Scanning Data. *IEEE Transactions on Intelligent*

Transportation Systems, Vol. 16, No. 1, 2015, pp. 194–205. https://doi.org/10.1109/TITS.2014.2328589.
41. Kumar, P., C. P. McElhinney, P. Lewis, and T. McCarthy. 2014. Automated Road Markings Extraction from Mobile Laser Scanning Data. *International Journal of Applied Earth Observation and Geoinformation*, Vol. 32, 2014, pp. 125–137. https://doi.org/10.1016/j.jag.2014.03.023.
42. Yu, Y., J. Li, H. Guan, F. Jia, and C. Wang. Learning Hierarchical Features for Automated Extraction of Road Markings From 3-D Mobile LiDAR Point Clouds. *IEEE Journal of Selected Topics in Applied Earth Observations and Remote Sensing*, Vol. 8, No. 2, 2015, pp. 709–726. https://doi.org/10.1109/JSTARS.2014.2347276.
43. Chen, X., B. Kohlmeyer, M. Stroila, N. Alwar, R. Wang, and J. Bach. 2009. Next Generation Map Making: Georeferenced Ground-Level LIDAR Point Clouds for Automatic Retroreflective Road Feature Extraction. *In Proceedings of the 17th ACM SIGSPATIAL International Conference on Advances in Geographic Information Systems*, GIS '09, 488–491. Association for Computing Machinery, New York, 2009.
44. Yang, B., Y. Liu, Z. Dong, F. Liang, B. Li, and X. Peng. 3D Local Feature BKD to Extract Road Information from Mobile Laser Scanning Point Clouds. *ISPRS Journal of Photogrammetry and Remote Sensing*, Vol. 130, 2017b, pp. 329–343. https://doi.org/10.1016/j.isprsjprs.2017.06.007.
45. Yang, B., Z. Dong, Y. Liu, F. Liang, and Y. Wang. Computing Multiple Aggregation Levels and Contextual Features for Road Facilities Recognition Using Mobile Laser Scanning Data. *ISPRS Journal of Photogrammetry and Remote Sensing*, Vol. 126, 2017a, pp. 180–194. https://doi.org/10.1016/j.isprsjprs.2017.02.014.
46. Jung, J., E. Che, M. J. Olsen, and C. Parrish. Efficient and Robust Lane Marking Extraction from Mobile LIDAR Point Clouds. *ISPRS Journal of Photogrammetry and Remote Sensing*, Vol. 147, 2019, pp. 1–18. https://doi.org/10.1016/j.isprsjprs.2018.11.012.
47. Rastiveis, H., A. Shams, W. A. Sarasua, and J. Li. Automated Extraction of Lane Markings from Mobile LiDAR Point Clouds Based on Fuzzy Inference. *ISPRS Journal of Photogrammetry and Remote Sensing*, Vol. 160, 2020, pp. 149–166. https://doi.org/10.1016/j.isprsjprs.2019.12.009.
48. Zhang, D., X. Xu, H. Lin, R. Gui, M. Cao, and L. He. Automatic Road-Marking Detection and Measurement from Laser-Scanning 3D Profile Data. *Automation in Construction*, Vol. 108, 2019, 102957. https://doi.org/10.1016/j.autcon.2019.102957.
49. Ai, C., and Y. J. Tsai. An automated Sign Retroreflectivity Condition Evaluation Methodology Using Mobile LIDAR and Computer Vision. *Transportation Research Part C: Emerging Technologies*, Vol. 63, 2016, pp. 96–113. https://doi.org/10.1016/j.trc.2015.12.002.

50. Tsai, Y. J., and Z. Wang. Validating Change of Sign and Pavement Conditions and Evaluating Sign Retroreflectivity Condition Assessment on Georgia's Interstate Highways Using 3D Sensing Technology. 141. *Georgia DOT*, Atlanta, 2019.
51. ASTM International. ASTM E1710-18 Standard Test Method for Measurement of Retroreflective Pavement Marking Materials with CEN-Prescribed Geometry Using a Portable Retroreflectometer. *ASTM*, West Conshohocken, PA, 2018.
52. Mahlberg, J. A., Y.-T. Cheng, D. M. Bullock, and A. Habib. 2021. Leveraging LiDAR Intensity to Evaluate Roadway Pavement Markings. Future Transportation, Vol. 1, No. 3, 2021, pp. 720–736. https://doi.org/10.3390/futuretransp1030039.
53. Otsu, N. A Threshold Selection Method from Gray-Level Histograms. *IEEE Transactions on Systems, Man, and Cybernetics*, Vol. 9, No. 1, 1979, pp. 62–66. https://doi.org/10.1109/TSMC.1979.4310076.